

## 5. TESTING

### 5.1 Test Planning

The basic objectives of the PCCV test were specified by NUPEC in the Master Project Plan [34]. The stated objective of this plan was to... “investigate the ultimate behavior of PCCV under pressure beyond the design basis accident and to prove the pressure retaining capacity of PCCV.” NUPEC originally specified a series of five tests, illustrated in Figure 5.1: 1) trial pressurization to 0.4 kg/cm<sup>2</sup> (5.7 psig or 0.1 P<sub>d</sub>), 2) structural integrity and integrated leak rate tests to 4.5 and 3.6 kg/cm<sup>2</sup> (64.1 and 51.2 psig or 1.125 and 0.9 P<sub>d</sub>), respectively, 3) two design pressure tests to 4.0 kg/cm<sup>2</sup> (57 psig or 1.0 P<sub>d</sub>), and 4) a Limit State Test (LST) terminating with excessive leakage or structural failure.

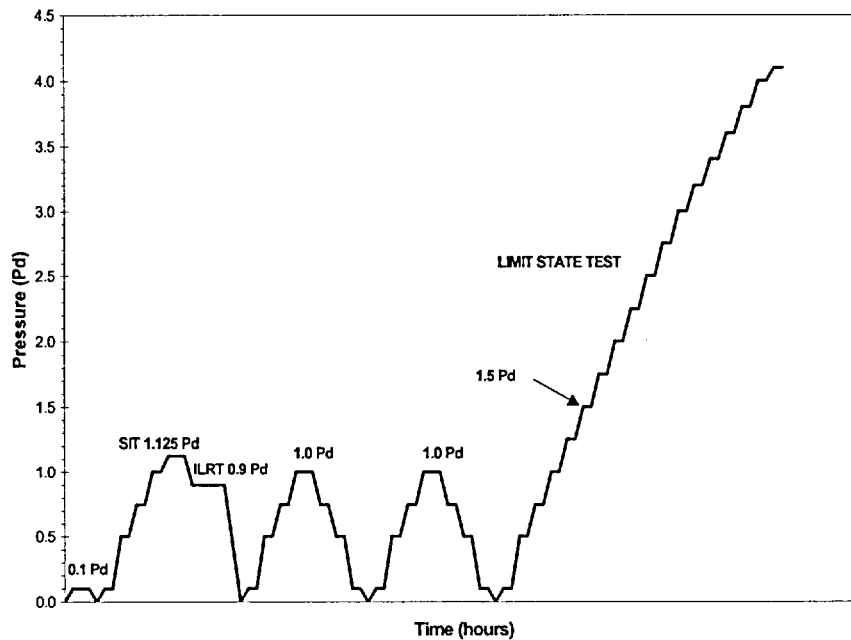


Figure 5.1 Original Pressurization and Depressurization Sequence [34]

After extensive discussions between NUPEC, the NRC and SNL, a detailed Test Plan [35] was developed by SNL to describe the conduct of the PCCV model's pressurization tests. Additional procedures that addressed the safe conduct of the tests were defined in the Operating Procedure [36]. The Test Plan includes:

- procedures to be conducted prior to tests to assure that all systems are ready;
- a list of test personnel required to conduct the tests and an outline of functions and checklists assigned to each person;
- procedures to be followed during the tests, including the general test philosophy;
- procedures to be conducted after pressure tests are completed.

Detailed checklists were prepared to ensure that all test operations were conducted as planned and completed in the appropriate sequence. Detailed procedural logs, stored in the project files, were generated to document the conduct of each test. A summary of the test plan is included in this chapter.

A final series of three tests were agreed upon. These tests are defined as follows and are illustrated in Figure 5.2.

1. A leak check and System Functionality Test (SFT) at 0.5 P<sub>d</sub> (2.0 kg/cm<sup>2</sup> or 28.4 psig)

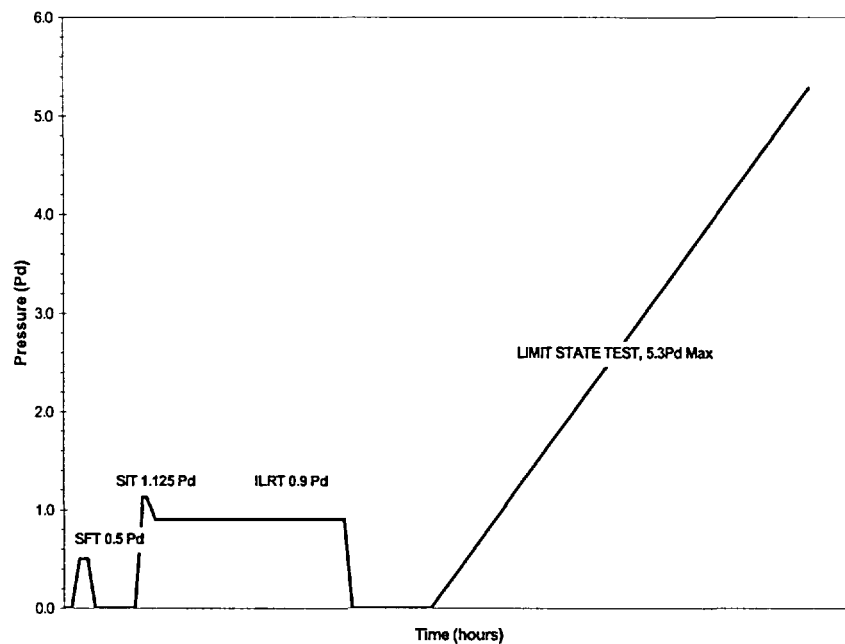


**Figure 5.2 Final Pressurization Plan**

2. A Structural Integrity Test (SIT) at  $1.125 P_d$  followed by an Integrated Leak Rate Test (ILRT) at  $0.9 P_d$
3. An Limit State Test (LST) to the static pressure capacity of the PCCV model (or the pressurization system, whichever comes first)

A fourth test was added to the test program after the conclusion of the LST. After careful evaluation of the LST results, NUPEC, the NRC, SNL, and their technical advisors concluded that not all of the program's objectives were met after the LST. SNL was tasked with designing and conducting a test that would allow the PCCV model to be pressurized beyond the level reached during the LST in an attempt to observe greater inelastic response of the model and, hopefully, generate a structural failure mode. This Structural Failure Mode Test (SFMT) is described in Section 5.2.4.

#### 5.1.1 Pressurization System Design and Operation

The pressurization system for the PCCV model test consisted of a pressure source, a valve gallery (consisting of several valves, a flow meter, and several sensors) used to control the flow of nitrogen, a programmable logic controller (PLC), control computer, and high pressure piping which interconnects all the components. A schematic of the pressurization system is shown in Figure 5.3

For the SFT, SIT/ILRT, and SFMT, the pressure source consisted of a pressurized nitrogen tube trailer. The trailer was located adjacent to the PCCV model, next to the valve gallery with a short flexible hose connecting them. For the LST, the pressure source consisted of a truck with liquid nitrogen that was gasified and regulated to a constant pressure and temperature. This source was located more than 600 m (2000') away from the PCCV model for safety reasons, near Building 9950. The pressurized nitrogen gas was piped aboveground onto the CTTF site and into the valve gallery.

In addition to the temperature being controlled at the source location during the pressure testing, the gas was heated in the piping prior to entering the PCCV model. These heaters helped increase the temperature of the gas prior to entering the PCCV model. Several additional heaters were located inside the model to help maintain temperatures to within  $\pm 5$  degree C of the average ambient temperature ( $\sim 15^\circ \text{C}$ ) outside the PCCV model.



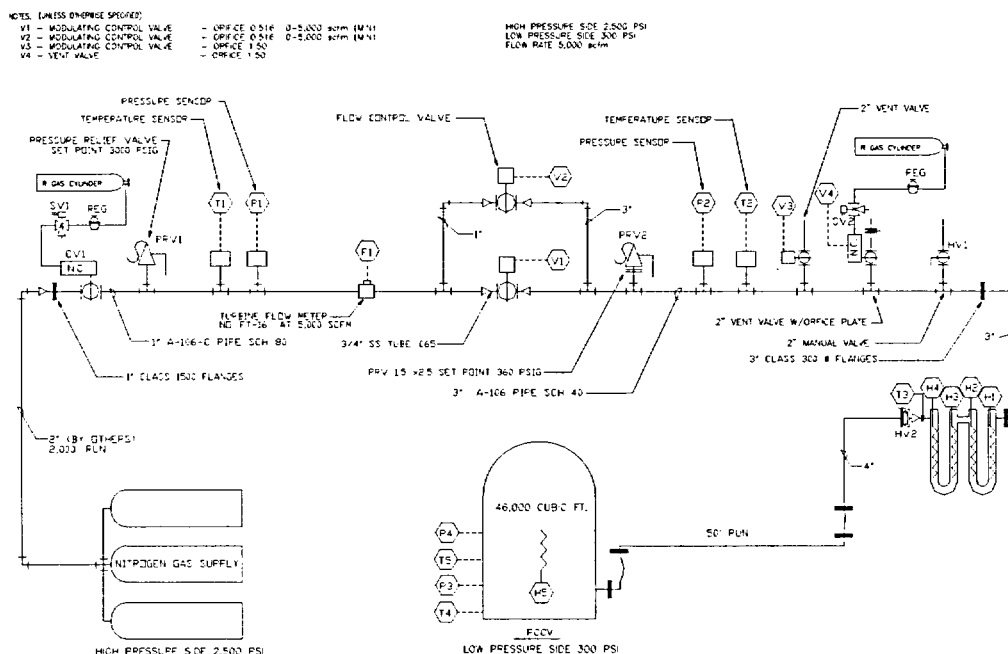


**Figure 5.3 Pressurization System Schematic**

The pressurization system was controlled by the PLC, which was located on the valve gallery skid next to the PCCV model. Communication with the PLC was performed by the control computer located in Building 9950. A more detailed description of the entire pressurization system is provided in the PCCV Pressurization System Data Package [37].

The entire pressurization system was designed and fabricated by an outside contractor (Rupert Plumbing and Heating Company, Inc., Albuquerque, NM). Initial testing of the system (primarily the valve gallery and heaters) was performed by the contractor prior to delivery to the CTTF site. After the system was installed at the site, the system was tested again before connecting to the PCCV model and conducting the pressure tests of the model.

The system tests performed by the contractor were approved by SNL personnel and encompassed all possible conditions the system might have to deal with during both the low- and high-pressure testing. These system tests checked all wiring, valve functionality, instrument functionality, and the control hardware and software.

After the system was installed and tested, the piping into the PCCV model was hooked up. All pressure lines connected to the valve gallery and the PCCV model were clean and dry before they were connected. Before the flex hose and flange were connected to the PCCV model, the line was "blown out" to clean it. The pressure source line up to the valve gallery was also blown out prior to the final hook-up.

## 5.2 Test Operations

The over-pressurization tests of the PCCV model were conducted at the CTTF-W, shown in Figure 1.3.

Building 9950, an ancillary facility for the test site (shown in the background in Figure 2.11), was the headquarters for conducting the pressure tests. It housed the control room and the observation room. During the test, key project members were inside the control room to execute the test plan and monitor the response of the model. Visitors observed the test progress and received periodic information on test status in the observation room.

The basic test team for each test is shown in Figure 5.4. The test team was only fully staffed for the LST and the SFMT. Test staffing for prestressing and the low-pressure tests is shown in Table 5.1.

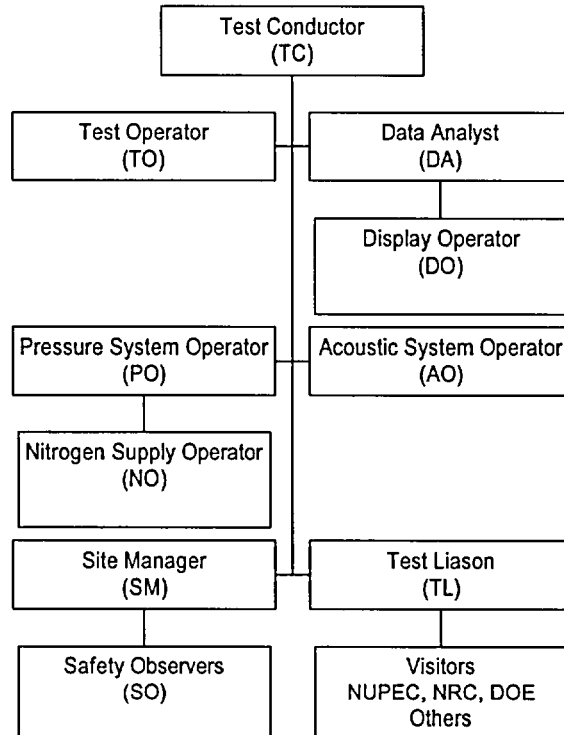


**Figure 5.4 PCCV Test Organization**

**Table 5.1 PCCV Test Personnel Matrix**

Position	Prestressing	SFT	SIT/ILRT	LST	SFMT
Test Conductor	X*	X	X	X	X
Test Operator	X	X	X	X	X
Data Analyst				X	X
Display Operator			X	X	X
Pressure System Operator		X	X	X	X
Acoustic System Operator	X	X	X	X	X
Site Manager	X	X	X	X	X
Safety Observers			X	X	X
Nitrogen Supply Operators		X	X	X	X
Test Liaison			X	X	
Visitors			X	X	X

\*Part-time

### 5.2.1 System Functionality Test

The system functionality test and leak check was designed to verify the functionality of all the systems (instrumentation, data acquisition, pressurization, etc.) and the initial leak-tightness of the PCCV model (especially the sealing of the penetrations) prior to the performance of the pressure tests. Controlled leak tests were included to determine the accuracy of the leak detection instrumentation during the ILRT and LST.

The SFT was conducted beginning approximately 9:00 AM, July 18, 2000. The model was pressurized using nitrogen to 0.5  $P_d$  (0.2 MPa or 28.4 psig) in three increments holding pressure for one hour or longer at each step, depending on the duration needed to perform all system functionality and leak checks. The model was then isolated and a leak rate check was performed by monitoring the model pressure and temperature for approximately 18 hours. After 18 hours, the calculated leak rate was 0.15% mass/day, which confirmed that the model was leak-tight. After the model leak rate check, the model was allowed to depressurize through a pair of orifice plates calibrated to leak rates of 1% and 10% mass/day to perform a calibration test on the leak rate measurement instrumentation. The calculated leak rates for each test were 0.87% and 7.86%, respectively, indicating that the leak rate instrumentation accurately detected a leak of 1% mass per day, which is the goal specified for the ILRT. The SFT was concluded on July 20 by opening the vent valve, allowing the model to depressurize. The SFT pressure time history and leak rates are shown in Figures 5.5 and 5.6.

## 5.2.2 Structural Integrity Test and Integrated Leak Rate Test

The SIT and the ILRT were conducted on September 12-14, 2000 as a combined test, with the ILRT following immediately after the SIT. The SIT/ILRT reproduced the preoperational tests conducted at the prototype plant and allows for a comparison of the model's elastic response characteristics and leak behavior with the prototype and pretest analyses. The pressure and average temperature time histories measured during the test are shown in Figure 5.7.

### 5.2.2.1 Structural Integrity Test

The SIT followed the procedures specified by Japanese Standard JEAC 4203-1994 [38] and the ASME Boiler and Pressure Vessel Code, Section III, Division 2, Article CC-6000, "Structural Integrity Test of Concrete Containments." [9]

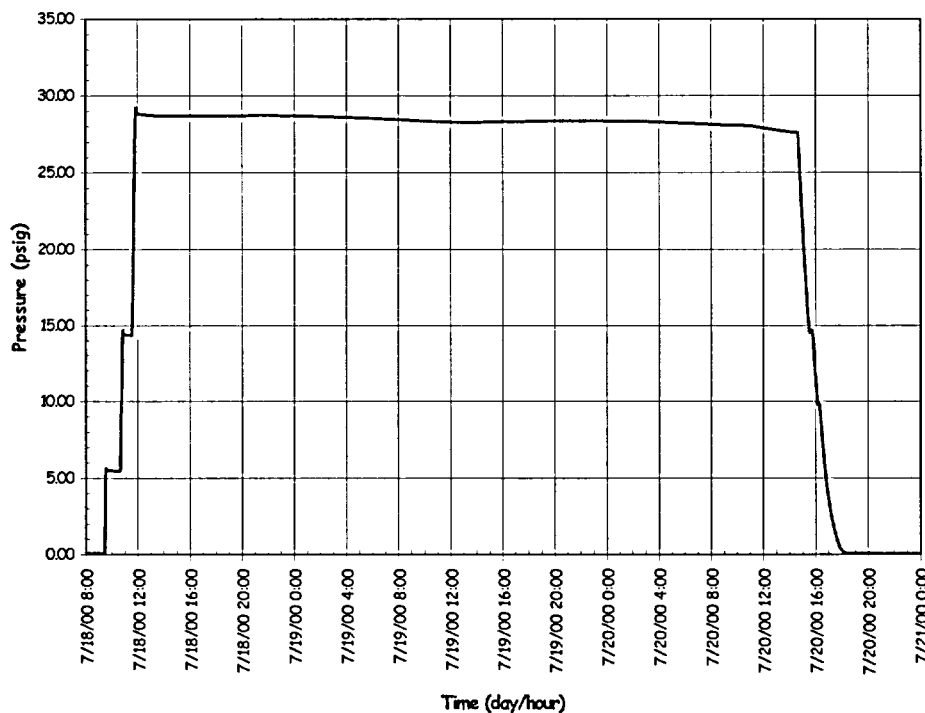


Figure 5.5 System Functionality Test Pressure Time History

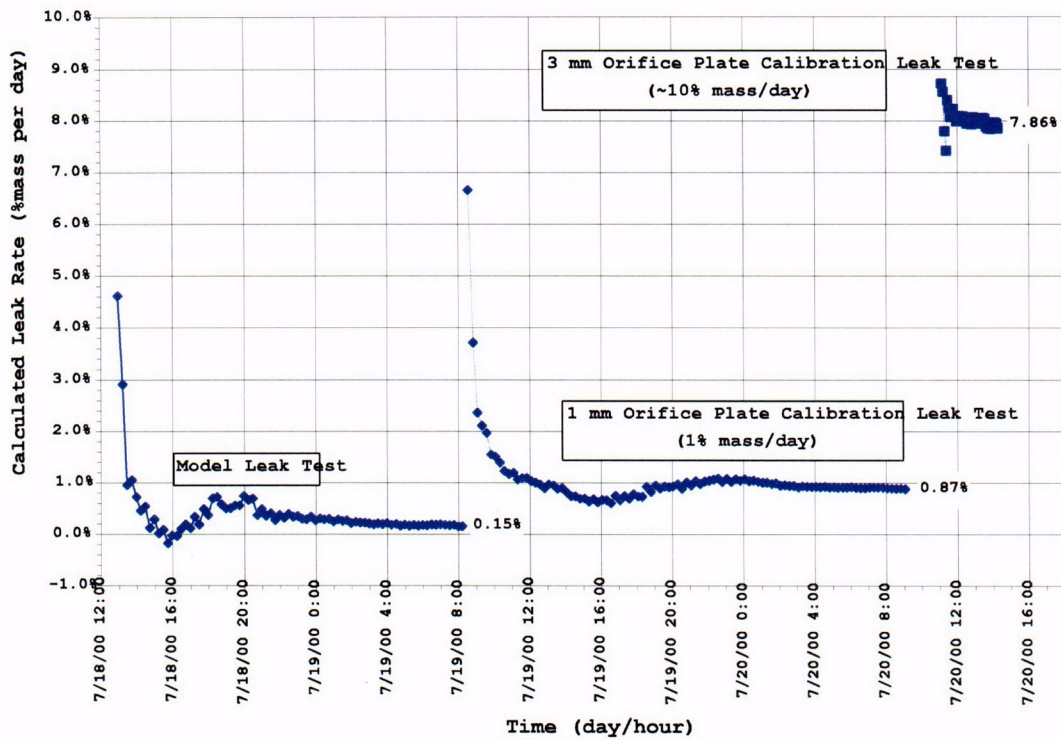


Figure 5.6 System Functionality Test Leak Rates

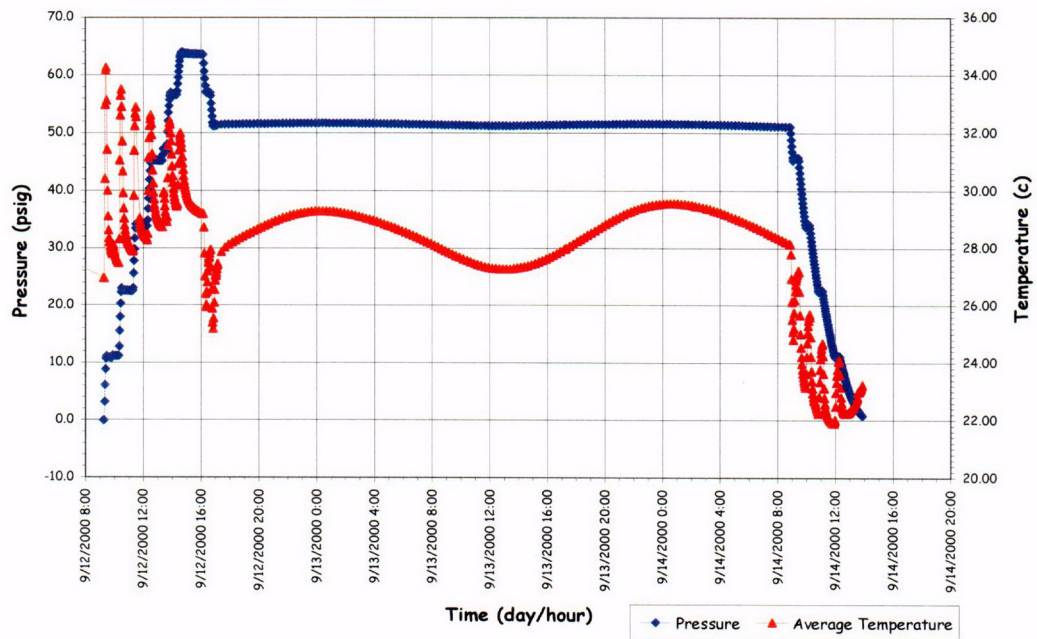


Figure 5.7 Structural Integrity and ILRT Pressure and Temperature Time Histories

Per MITI Code 501, Article 104 [39], the SIT test pressure,  $P_{SIT}$ , was  $1.125 P_d$  (0.44 MPa or 64 psig). The PCCV model was pressurized in five equal increments at a rate of 20% of the test pressure per hour. (CC-6110 requires pressurization to  $1.5 P_d$ .) Per CC-6340, the response of the model was recorded at each pressure step (including  $0 P_d$ ). Data of Record (DOR) was recorded when the following stability criterion was achieved:

$$\frac{Q_t - Q_{t-\Delta t}}{Q_{t-\Delta t}} \leq 0.02 \quad (5.1)$$

where  $Q_t$  and  $Q_{t-\Delta t}$  are the data at the current and the previous time interval, respectively. The next pressure increment followed only after this criterion was satisfied or the total step duration reached one hour.

All active gages in or on the model were recorded at each step. The locations of the gages were selected to allow for direct comparison of the PCCV model response to the prototype at the SIT pressure in addition to the primary objective of monitoring the response of the model to ultimate pressure. Table 5.2 summarizes the ASME code requirements for SIT measurements.

**Table 5.2 Summary of ASME B&PV Code SIT Instrumentation Requirements**

	Measurements	Accuracy/Range	Pressure	Acceptance Criteria
Cracking	CC-6350 Cracks > 0.01"x 6" @ specified locations	CC-6225 >0.005" @ 0.003"	CC-6350 Before test @ $P_{SIT}$ After test	CC-6420 Review by Designer
Strains	CC-6370: (Concrete Strains) @ Wall/Slab @ E/H @ Shell Discontinuities @ Restraints @ Steel/Concrete Trans.	CC-6224 $\pm 5\% \epsilon_{max}$ or $10 \mu\epsilon$ Gage Length > 4"	CC-6371 1. Baseline-Continuously for 24 hrs prior to test CC-6340 2. @ $P_0$ (Atmospheric press.) 3. During pressurization @ 20% $P_{SIT}$ 40% $P_{SIT}$ 60% $P_{SIT}$ 80% $P_{SIT}$ 100% $P_{SIT}$ 4. @ PSIT + 1 hour 5. During depressurization @ 80% $P_{SIT}$ 60% $P_{SIT}$ 40% $P_{SIT}$ 20% $P_{SIT}$ @ $P_0$	CC-6410 (a) No rebar yielding (b) No visible liner or concrete damage  (c-2) Residual displacements: @ Pts of Max. $\delta_R$ & $\delta_V$ : $\delta_{res} < 20\% \delta_{max} * @ P_{SIT} + 0.01"$ (*measured or predicted) Avg. $\delta_R$ @ each elevation: $\delta_{res} < 20\% \delta_{max} * @ P_{SIT} + 0.01"$
Displacements	CC-6361: $\delta_R$ @ 20%H & 0°, 90°, 180°, 270° $\delta_R$ @ 40%H & 0°, 90°, 180°, 270° $\delta_R$ @ 60%H & 0°, 90°, 180°, 270° $\delta_R$ @ 80%H & 0°, 90°, 180°, 270° $\delta_R$ @ 100%H & 0°, 90°, 180°, 270° $\delta_R$ @ E/H (12 points) $\delta_V$ @ Springline & 0°, 90°, 180°, 270° $\delta_V$ @ Apex $\delta_V$ @ two pts. Bet. Apex & Springline	CC-6223 $\pm 5\% \delta_{max}$ or 0.01"		
Temperature	CC-6380 Concrete @ Specified locations for Strain Correction Gas @ Interior & Exterior	CC-6226 $\pm 2^\circ F$ Range: Expected temp.		
Pressure		CC-6222: $\pm 2\% P_{SIT}$ Range < 4 $P_{SIT}$		

In general, the model instrumentation satisfied all of the requirements summarized in Table 5.2 with the following exceptions or modifications.

- The entire surface of the cylinder was mapped for cracks prior to the test; however, crack widths were not measured. No crack mapping was performed during the SIT. After the SIT, additional cracks within selected areas of the cylinder wall were identified but the widths were not measured. The crack map grid is shown in Figure 5.8
- Model strains were measured primarily using the gages mounted directly to the rebar and liner. Only a limited number of concrete strains were measured directly.
- Displacements were measured at all specified locations with the exception of the points around the largest penetration (i.e. the E/H)

Figure 1. Schematic representation of the experimental design. The subjects were divided into two groups: a control group and an experimental group. The control group received a standard training program, while the experimental group received a modified training program. The experimental group was further divided into two subgroups: a low-intensity group and a high-intensity group. The low-intensity group received a low-intensity training program, while the high-intensity group received a high-intensity training program. The subjects were then subjected to a series of tests to measure their performance and physiological responses.



After the SIT pressure was maintained for the required minimum of one hour per CC-6320, the PCCV model was depressurized to the ILRT pressure. First, the model was depressurized to Pd, for comparison with the pressurization phase, before depressurizing to the ILRT pressure (0.9Pd).

The temperature inside the model was specified to be maintained at approximately 25 °C (77 °F) during the test with a maximum range of 10 °C to 38 °C (50 °F to 100 °F). The average temperature during the SIT, recorded by the RTDs, was closer to 30 °C (86 °F). The ambient air temperature outside the model was measured near the base of the model.

### 5.2.2.2 Integrated Leak Rate Test

The ILRT requirements for Japanese containments are specified in JEAC 4203-1994 [38]. The ILRT requirements for U.S. containment vessels are specified in 10CFR50, Appendix J “Primary Reactor Containment Leakage Testing for Water-Cooled Power Reactors,” [40] which references the tests procedures in American National Standards ANSI/ANS N45.2-1974 “Leakage Rate Testing of Containment Structures for Nuclear Reactors [41] and ANSI/ANS N56.9-1987 “Containment System Leakage Testing Requirements.” [42]

The ILRT for the PCCV model was a hybrid of these procedures. The ILRT pressure,  $P_{ILRT}$ , was 0.9 Pd (0.35 MPa or 51.2 psig) based on JEAC 4203 and the Absolute Method for a Type A Test per ANSI/ANS N56.9 (Section 5.0) was followed. After depressurizing from the  $P_{SIT}$  to  $P_{ILRT}$ , the model was held at  $P_{ILRT}$  for approximately one hour to allow the model atmosphere to stabilize before the start of the leakage rate test. The ILRT commenced after all stabilization criteria were achieved and the duration of the test was “sufficient to enable adequate data to be accumulated and statistically analyzed so that a leakage rate ... can be accurately determined” but no less than 24 hours. Data was collected at least once every hour. The measured leakage rate at  $P_{ILRT}$ ,  $L_{tm}$ , was determined using both the (a) total time analysis and (b) point-to-point analysis techniques. The nominal atmospheric pressure at the elevation of the test site (verified by checking the Sandia Photovoltaics Weather Station reading) was used for leak rate calculations. The calculated leak rate after 24 hours at 0.9  $P_d$ , was 0.059% mass/day.

After the ILRT was completed, the model was initially depressurized by venting through the 1mm orifice plate, calibrated for a leak rate of 1% mass/day. After approximately 16 hours, a stable leak rate of 0.996% mass per day was calculated, again confirming the accuracy of the leak rate instrumentation.

The calculated leak rates during and after the ILRT are shown in Figure 5.9.

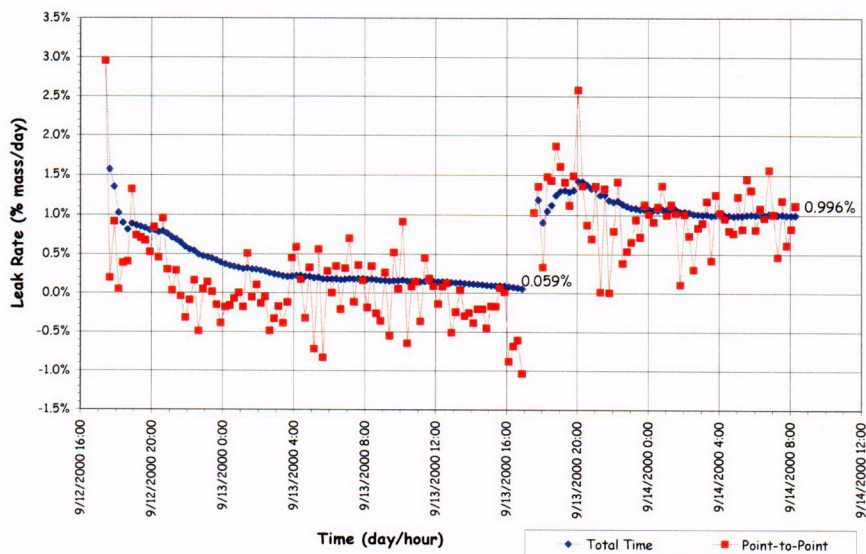


Figure 5.9 Integrated Leak Rate Test Leak Rates

Per JEAC 4203, the maximum leak rate at the ILRT pressure should be less than 0.1% mass/day. Similarly, per 10 CFR 50, the specified maximum allowable leak rate,  $L_a$ , at the design accident pressure,  $P_d$ , for the prototype containment is 0.1% mass/day. The maximum leak rate at the ILRT pressure level,  $L_i$ , is

$$L_i = L_a (P_{ILRT}/P_d) = 0.09\% \text{ mass/day}$$

Normally, the measured leak rate,  $L_{tm}$ , should be less than  $0.75L_i$  (0.07% mass/day). For the PCCV model, this translates into measuring a change in pressure of approximately  $0.001 \text{ kg/cm}^2$  (0.02 psi), which is beyond the capability of the instrumentation to resolve. While the calculated leak rates are within the limits specified in the standards, the accuracy of these leak rate estimates is questionable. Using the instruments selected for the high pressure test, however, the PCCV model exhibited a leak rate which was less than 1% mass/day, which corresponds to a pressure drop of 0.004 MPa (0.6 psi) over 24 hours.

While holding at the ILRT pressure, a limited amount of crack mapping was performed. This was accomplished by tracing all new cracks in predetermined areas and taking still photos of these areas. Cracks in the area to the left of the E/H prior to the SIT were traced in black and are shown in Figure 5.10. New cracks, traced in blue during the ILRT, are shown in Figure 5.11. Cracks widths were not measured.



Figure 5.10 Pre-SIT Cracks at Azimuth. 350 degrees, Elev. 4680 to 6200 (Grid 45)

Model response data was also recorded during and after the SIT/ILRT. Figures 5.12 and 5.13 show the radial and vertical displacement of the model as a function of time.

The initial displacements represent the net effect of prestressing, creep, shrinkage, etc. from the 'zero' reading in March to the start of the SIT in September. The cyclic response during the ILRT is an indication of the model's response to variation in ambient temperature and direct heating.

After the leak rate calibration, the PCCV model was depressurized at approximately the same rate and increments as the initial pressurization phase to compare the responses at the same pressure levels.

An exclusion zone was established for the SIT, consisting of a circular area with radius of 600 m (2,000'), centered at the PCCV model. The exclusion zone, as shown in Figure 5.14, was marked, and signs were posted to identify this area. The safety observers monitored the exclusion zone at all times during the test to make sure that no intruder entered this area. No exclusion zone was required for the ILRT because the model pressure was below the design pressure ( $0.9P_d$ ).



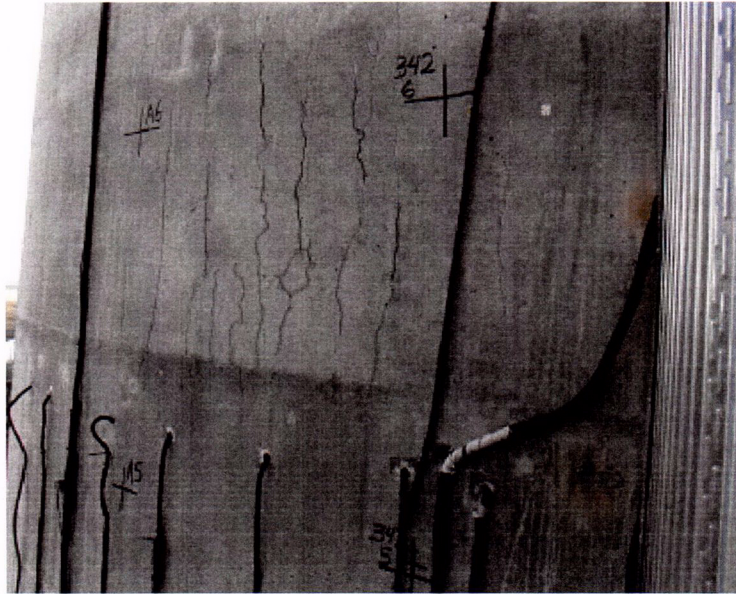


Figure 5.11 Post-SIT Cracks at Azimuth. 350 degrees, Elev. 4680 to 6200 (Grid 45)

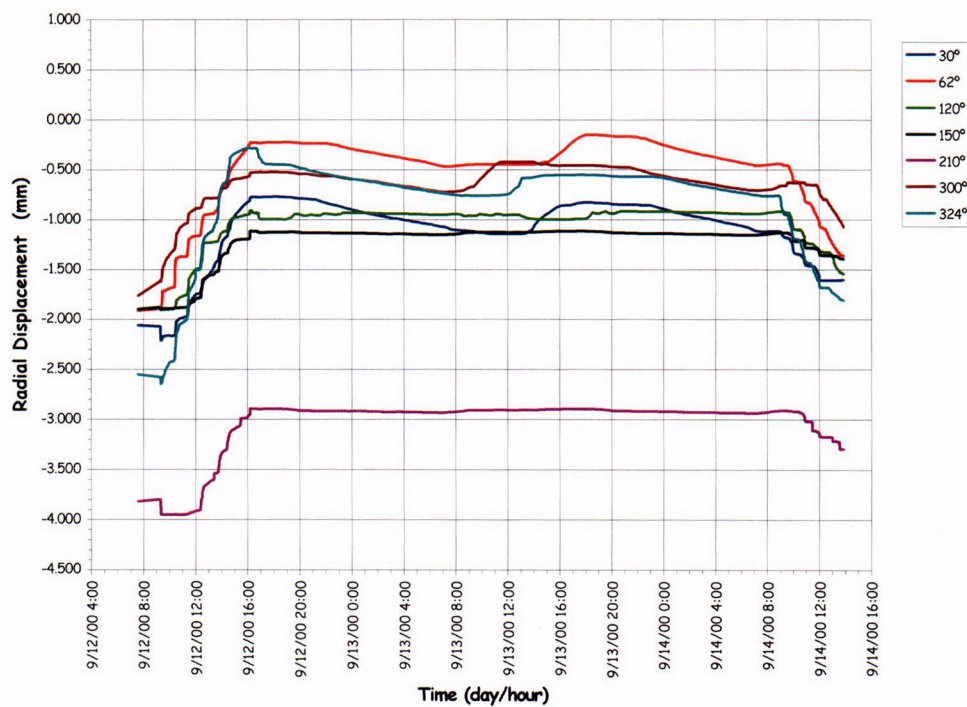


Figure 5.12 SIT/ILRT Radial Displacements at Cylinder Midheight (Elev. 4680)

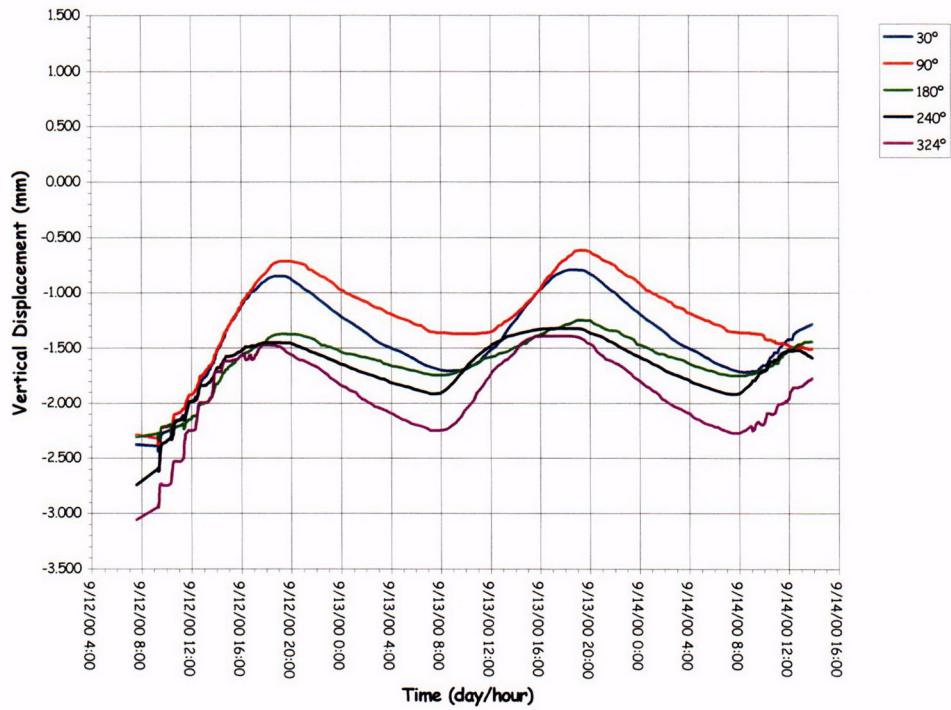


Figure 5.13 SIT/ILRT Vertical Displacements at Springline (Elev. 10750)

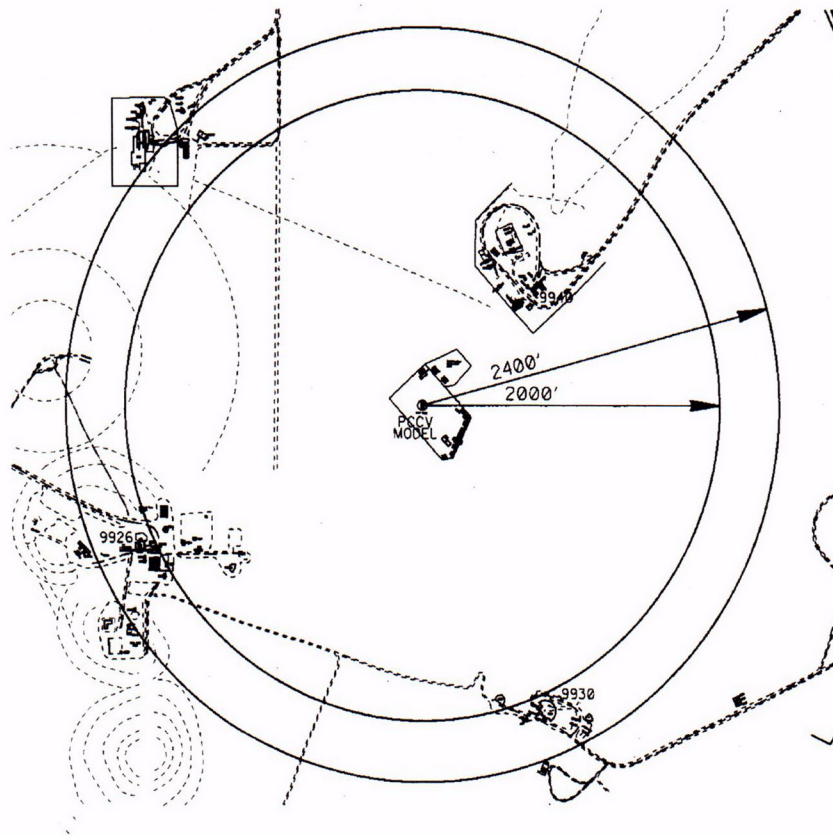


Figure 5.14 PCCV SIT/ILRT, LST, SFMT Exclusion Zone



Personnel were permitted to approach the model after the pressure has stabilized and the test conductor (TC) determined that it was safe to approach the model.

### 5.2.3 Limit State Test

The LST was designed to fulfill the primary objectives of the PCCV test program, i.e. to investigate the response of representative models of nuclear containment structures to pressure loading beyond the design basis accident and to compare analytical predictions to measured behavior. The LST was conducted after the SIT and ILRT were completed and the data from these tests evaluated. The PCCV model was depressurized between the SIT/ILRT and the LST. The LST began at 10:00 AM, Tuesday, September, 26, 2000, and continued, without depressurization, until the test was terminated just before 5:00 PM on Wednesday, September 27.

The exclusion zone for the LST covered the same circular area of radius 600 m (2,000'), centered at the PCCV model, as shown in Figure 5.14. At this radius, the estimated peak free-field overpressure due to a sudden burst at an internal pressure 2.1 MPa or 300 psig [34] is 1.66 kPa (0.24 psi). This is below the free-field allowable whole body exposure of 3.4 kPa (0.5psi) specified by SNL Environmental Safety and Health (ES&H) regulations. The safety observers monitored the exclusion zone at all times during the LST to make sure no intruder entered this area. In addition, the safety observers monitored the area above the model for aircraft. If an aircraft had approached the exclusion zone, pressurization of the model would have been suspended or held until the aircraft cleared the exclusion zone.

The pressure and average temperature time histories during the LST, including depressurization, are plotted in Figure 5.15. The LST followed the planned pressurization sequence up to the point where the model began leaking.

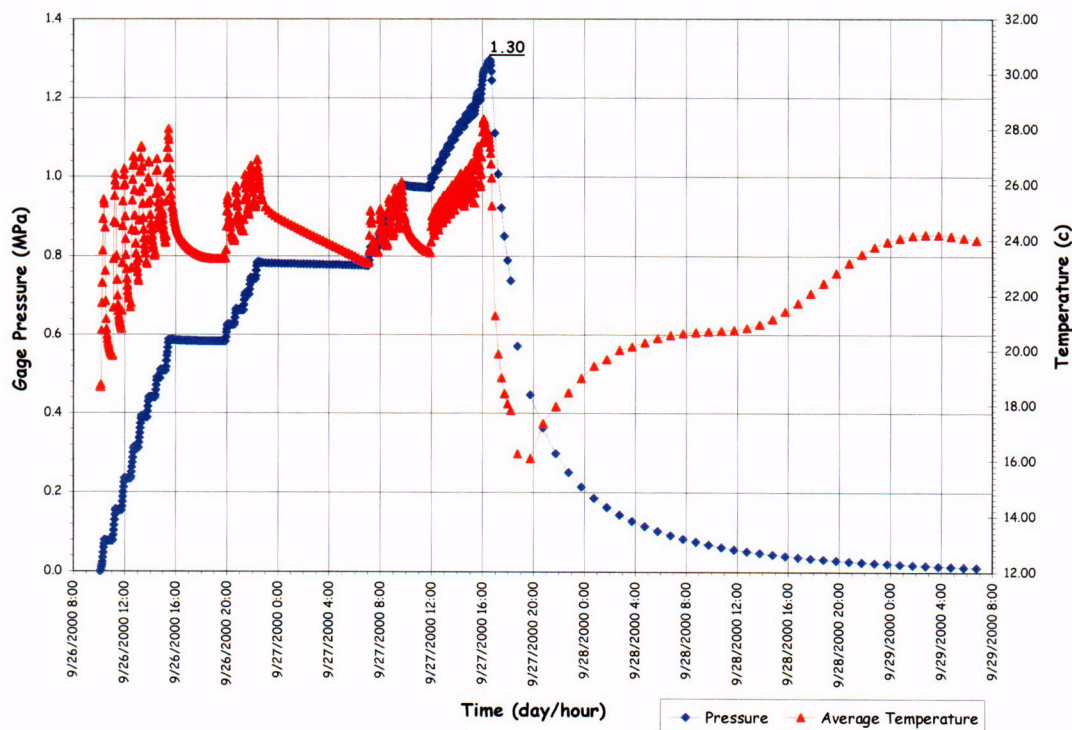


Figure 5.15 Limit State Test Pressure and Average Temperature

Initially, the model pressurization sequence matched the pressurization steps followed for the SIT to allow for comparison of the model response to two identical cycles of loading. The gage stability criteria used during the SIT (i.e. Equation 5.1) was also applied during the LST. Pressurization continued in increments of approximately  $0.2P_d$  until a pressure of  $1.5 P_d$  ( $6.0 \text{ kg/cm}^2$  or  $85.3 \text{ psig}$ ) was reached at approximately 4:30 PM. At this pressure, the first planned leak check was conducted by isolating the model and monitoring the temperature and pressure. After approximately three hours, a leak rate of 0.48% mass/day was calculated. Considering previous experience from the ILRT, which



demonstrated that thermal expansion of the model during the day yielded apparent leak rates in this range, the results were interpreted to indicate that the PCCV model was leak-tight.

Pressurization of the model continued in increments of approximately  $0.1P_d$  until a pressure of  $2.0P_d$  ( $8.0 \text{ kg}_f/\text{cm}^2$  or 113.8 psig) was reached at approximately 11:00 PM. At this pressure the model was again isolated to perform a planned leak check. This leak check was also planned to be held for 8 hours to allow the test team to partially stand down for a rest period. A 'skeleton crew' consisting of the TC, Data Acquisition System Operator (DO), and Nitrogen Supply Operator (NO) continued to monitor the response of the model and all other systems until approximately 7:00 AM on September 27. This pressure hold and leak check was also selected below the lower bound prediction for the onset of structural yielding (i.e. yielding of the rebar or tendons) to ensure the model would remain relatively stable during this period. After approximately eight hours, the calculated leak rate was 0.003%, i.e., essentially zero. This confirmed the interpretation of the leak check results at  $1.5 P_d$  and also demonstrated the greater accuracy of the leak rate results when the model is thermally stable.

Pressurization of the model resumed at 7:00 AM in increments of  $0.1P_d$ , with increasing dwell time between pressure steps (~30 minutes) required to meet the gage stability criteria. As the pressure was increased to the next planned leak check at  $2.5P_d$ , liner strain gages in the vicinity of the E/H (LSI-C-K5-12) began registering rapidly increasing strains in excess of 1%. At  $2.4P_d$  the acoustic system operator (AO) reported hearing a change in the acoustic output which might indicate that "something had happened." At approximately 10:00 AM at a pressure of  $2.5P_d$  ( $10.0 \text{ kg}_f/\text{cm}^2$  or 142.2 psig), the model was isolated for the third planned leak check. After approximately 1-1/2 hours, a fairly stable leak rate of 1.628% mass per day was calculated. The leak rate calculations at 1.5, 2.0, and  $2.5P_d$  are plotted in Figure 5.16. Coupled with the acoustic data that continued to confirm some new event had occurred, it became clear that the model was leaking, most likely from a tear in the liner in the vicinity of the E/H. Plots of the output of the four internal acoustic sensors surrounding the E/H at 2.3, 2.4, and  $2.5 P_d$  are shown in Figure 5.17.

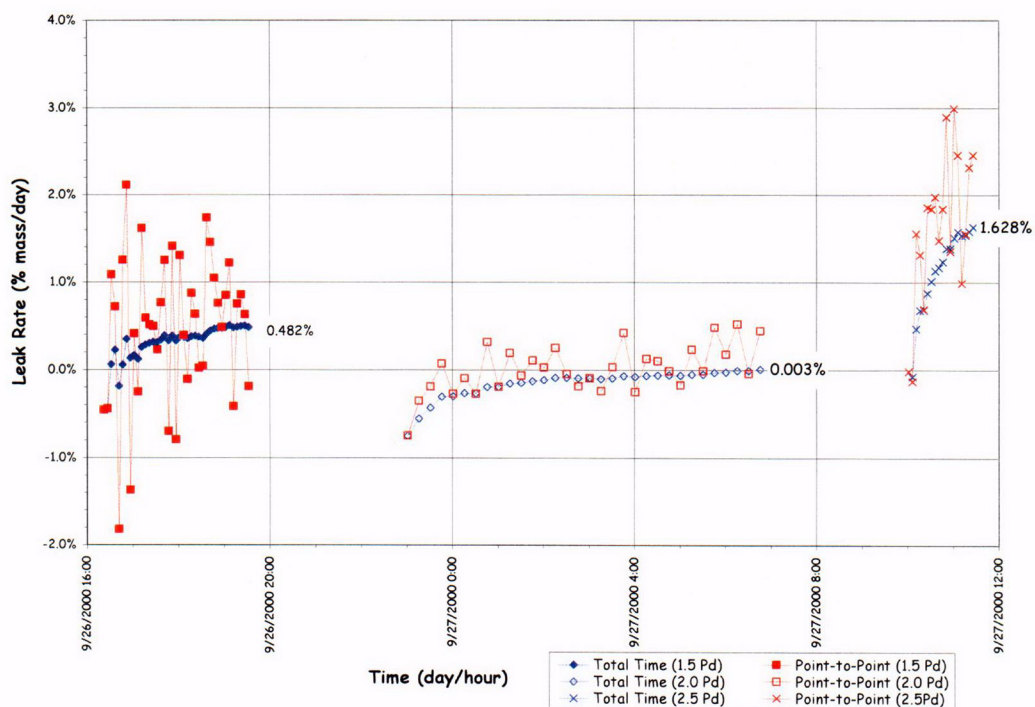


**Figure 5.16 LST Calculated Leak Rates at 1.5, 2.0 and  $2.5 P_d$**

After consulting with NUPEC and the NRC, the TC concluded that the model had functionally failed between 2.4 and  $2.5 P_d$  and directed a change in the pressurization plan. Since the model was leaking, the next goal was to pressurize the model as highly as possible to collect data on the inelastic response of the structure and to observe, if possible, a structural failure mode. Pressurization continued in increments of  $0.05 P_d$ , as planned. However, the gage stability criteria was abandoned and the hold time at each pressure step was reduced to less than 10 minutes.

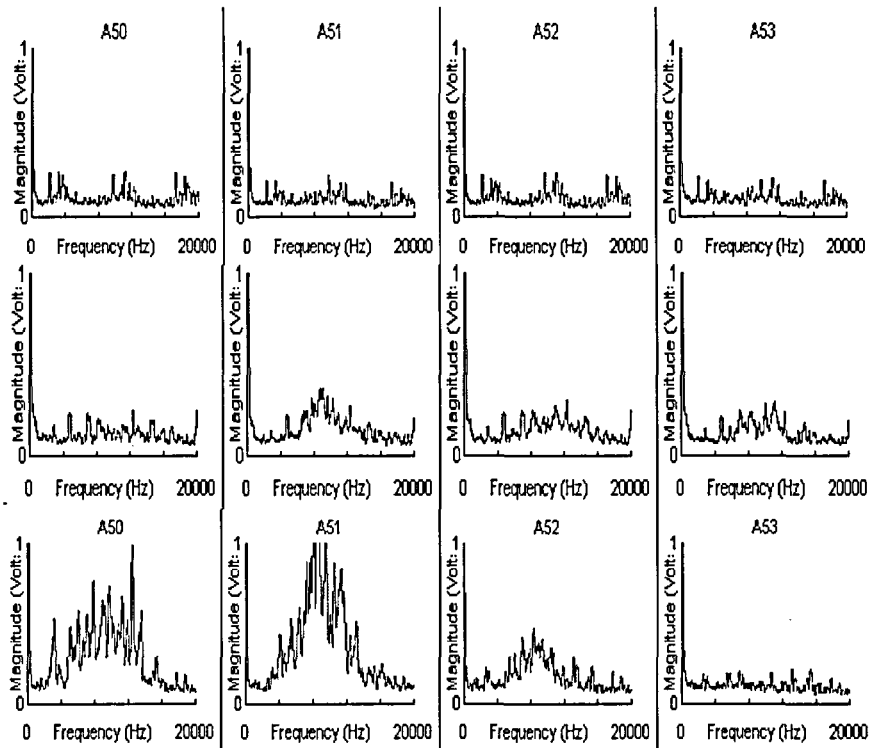


Figure 5.17 Internal Acoustic Sensor Signals at the E/H

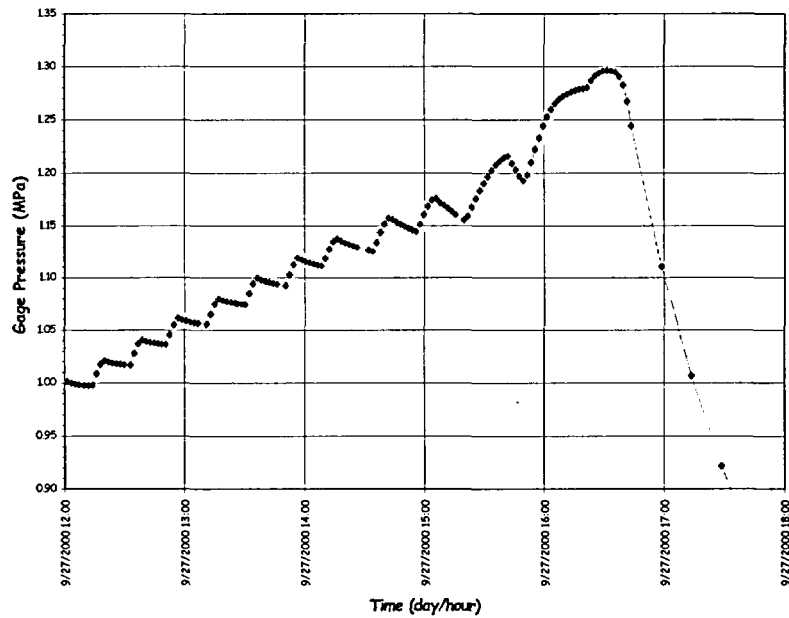
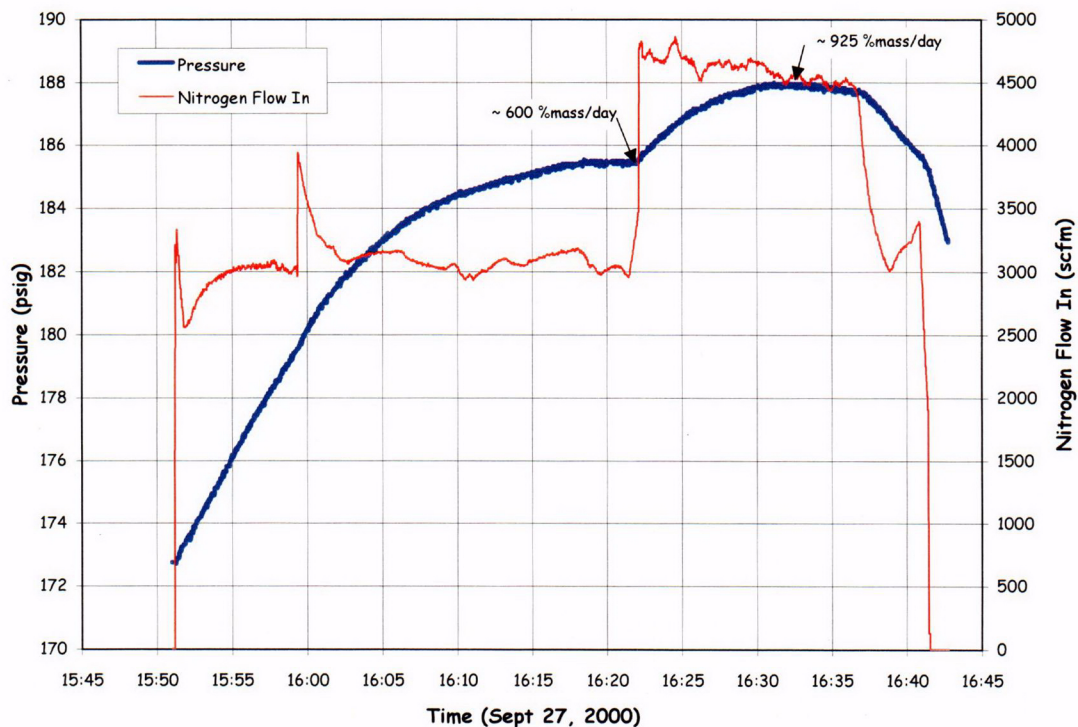


Figure 5.18 LST Pressure Time History, 2.5 to 3.3  $P_d$





**Figure 5.19 LST Pressure and Flow Rates at Maximum Pressure**

The PCCV model was pressurized to approximately  $3.0P_d$ , with increasing evidence of leakage and increasing liner strains. At  $3.0P_d$ , it became increasingly difficult to pressurize the model, and the nitrogen flow rate was increased to 99 std.m<sup>3</sup>/min (3500 scfm). At this flow rate, the pressure in the model was increased to  $3.1P_d$ . However, the pressure dropped steadily after reaching this pressure. The leak rate at this point was estimated to be 100%.

The nitrogen flow rate was increased to the maximum capacity of the pressurization system, 142 std.m<sup>3</sup>/min (5000 scfm), and the pressure was increased to slightly over  $3.3 P_d$  before the leak rate exceeded the capacity of the pressurization system. The pressure time history and flow rates during the final phase of the test are shown in Figures 5.18 and 5.19. Since it was no longer possible to increase the pressure in the model and the supply of nitrogen was nearly exhausted, the TC decided to begin terminating the test.

The isolation valve was closed and the model was allowed to depressurize on its own. The terminal leak rate was estimated to be on the order of 900% mass/day. (The maximum flow rate of nitrogen, 5000 scfm, is equivalent to a leak rate of 1000% mass/day.) Estimated leak rates during the final pressurization and depressurization phases are shown in Figures 5.20 and 5.21.

After the model pressure was reduced to  $1.0 P_d$ , test personnel were able to inspect the model close-up. Nitrogen gas was observed (heard and felt) escaping through many small cracks in the concrete around the penetration sleeves and at the tendon anchors. It was speculated that the liner acted as a leak chase, allowing nitrogen gas escaping through a tear or tears in the liner to travel between the liner and the concrete until it found an exit path through a crack in the concrete or a conduit in the tendon duct.

At maximum pressure, local liner strains of up to 6.5% were recorded and global hoop strains (computed from the radial displacement) at the mid-height of the cylinder averaged 0.4%. While large liner strains were observed, causing suspicion that the liner might have torn in several locations, the remainder of the structure appeared to suffer very little damage with the exception of more extensive concrete cracking at some locations. The largest crack was observed to the left of the E/H, shown in Figure 5.22. This is the same location as the crack photos shown in Figures 5.10 and 5.11. There was no indication of tendon or rebar failure. The detailed results of the LST are discussed in Section 5.3.2.1.

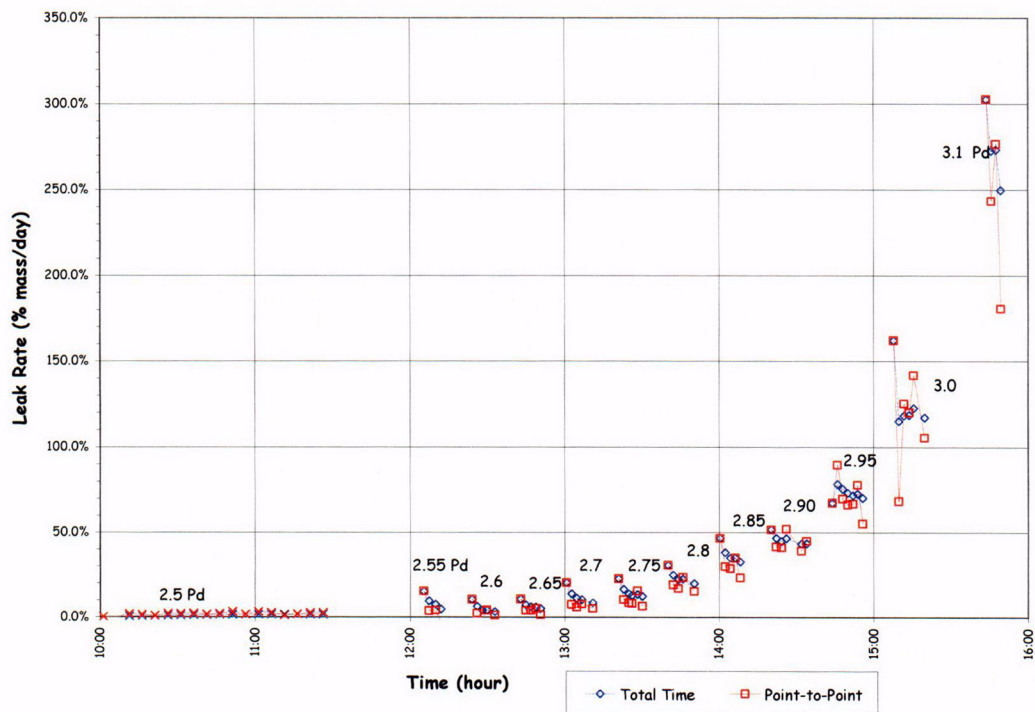


Figure 5-20. LST - Estimated Leak Rates (2.5-3.1 P<sub>d</sub>)

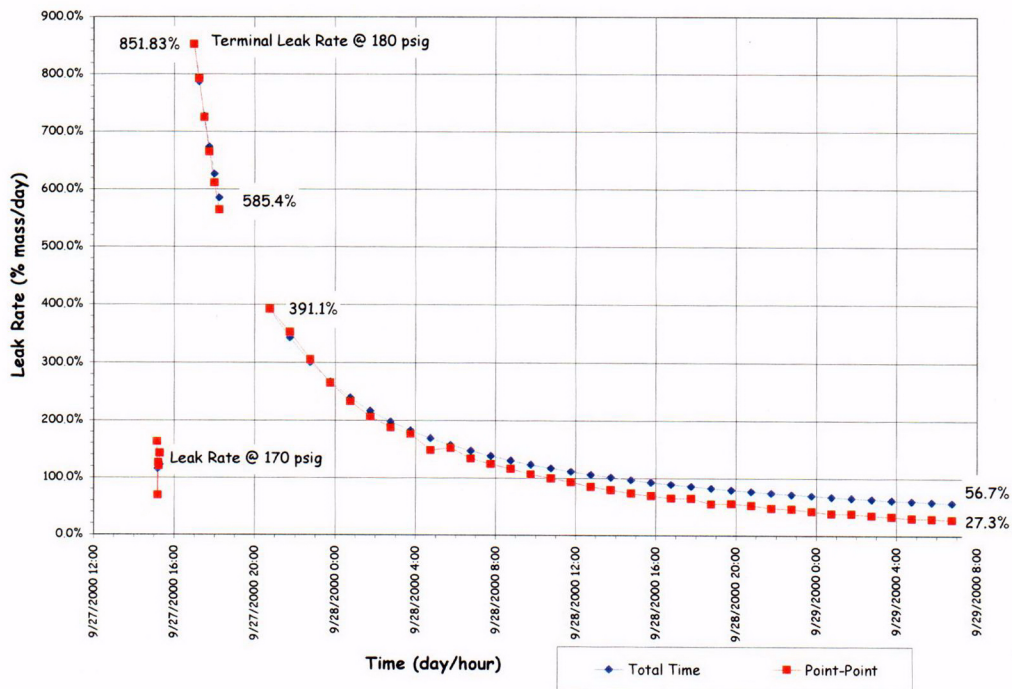


Figure 5.21 LST Estimated Terminal Leak Rates



Figure 5.22 Post-LST Cracks at Azimuth 350 degrees, Elev. 4680 to 6200 (Grid 45)

After the model had completely depressurized, it was purged with fresh air, the E/H was removed, and detailed posttest inspection of the inside of the model began. A cursory inspection of the model identified 26 discrete tears at 18 separate locations. A detailed posttest inspection plan was developed, and the results of this inspection are described in Section 5.3.2.1

#### 5.2.4 Structural Failure Mode Test

Almost immediately after the completion of the LST, it was recognized that while the PCCV model had demonstrated its capacity to resist pressures well above the design pressure and confirmed, arguably, liner tearing and leaking as the functional failure mode, the test objectives were not fully met with respect to observing large inelastic deformations for comparison with analyses, and witnessing the structural failure mode of the PCCV model. SNL was tasked by NUPEC and the NRC with investigating the possibility of conducting a second LST.

Two issues needed to be addressed to determine the technical feasibility of reloading the PCCV model. First was the question of whether the LST had caused damage to the structure such that any data obtained by reloading the structure would be compromised and of limited value for comparison with analytical results. The LST data was thoroughly reviewed and, with the exception of the liner and cracking of the concrete, there was no evidence of excessive structural damage. There was also no indication that the tendons had been strained beyond their yield limit and, except for a few isolated measurements, the same was true for the rebar. (Only 27 of the rebar gages registered strains in excess of 0.4% with a maximum of 1.7%—which likely reflects the local perturbation caused by the presence of the gage.) Comparing the radial displacement at the mid-height of the cylinder to the pretest Round Robin predictions in Figure 5.23 clearly illustrates that the structure was on the verge of global yielding but had not undergone a significant amount of inelastic



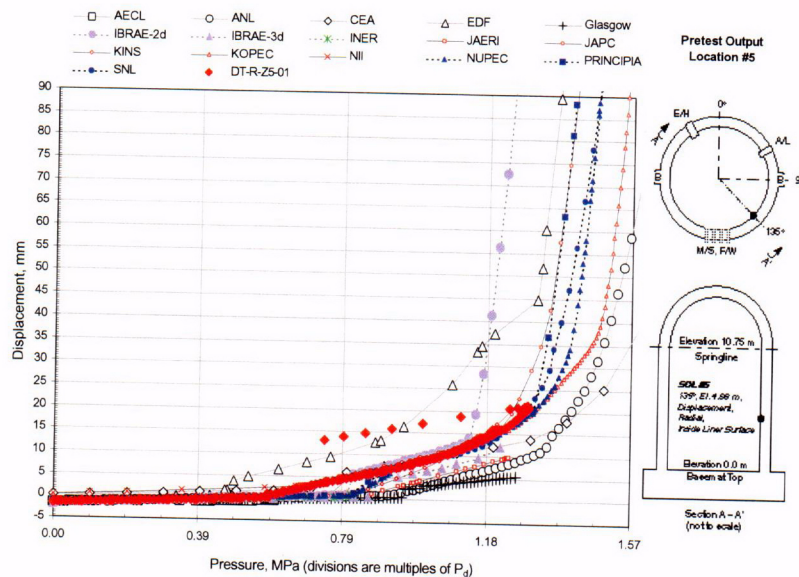


**Figure 5.23 LST Radial Displacement at Azimuth 135 degrees, Elev. 4680**

deformation. (In this context, only the yielding of the steel and rebar is addressed. Obviously, the loss in stiffness that occurs with global concrete cracking at approximately  $1.5P_d$  cannot be recovered.) This was a positive finding for the prospect of reloading the model since most, if not all, of the capacity of the rebar and tendons was still available. Another important conclusion from the consideration of the LST data was that if, in fact, the model was on the verge of global structural yielding, the additional pressure required to cause larger; inelastic deformations was not very large; perhaps only on the order of a few tenths to half the design pressure, i.e. an additional 1.0 to 2.0  $\text{kg}_f/\text{cm}^2$  (14 to 30 psig).

The second issue was the requirement to reseal the model in order to repressurize it. Since large sections of the liner were removed as part of the post-LST inspection, the liner was no longer capable of providing an effective membrane to prevent premature leakage. Furthermore, even if the liner tears and cutouts were locally repaired or sealed, it was clear that other areas of the liner were susceptible to tearing at the same pressures (or perhaps even at lower pressures) that caused the liner to tear during the LST. It was necessary, therefore, to devise a cost-effective method of completely replacing the liner function in order to proceed with plans to repressurize the PCCV. The replacement 'liner' was also required to ensure that the model could be repressurized to a level beyond the maximum pressure achieved during the LST. (A corollary of this conclusion was that there was no further need to investigate the response of the liner, and the instrumentation applied to the liner could be abandoned.)

Furthermore, the SFMT had to be completed within the current program budget and schedule. The concept developed to repressurize the PCCV model is illustrated in Figure 5.24.

The concept consists of sealing the interior surface of the liner with an elastomeric membrane after removing all interior transducers on the liner. After closing the E/H and A/L, the model would be filled with water to 1.5 m (5') from the dome apex, approximately 97% of the interior volume 1,591,000 ltr (350,000 gal). Filling the model with water would provide several advantages:

1. The leak rate of water through any tears in the liner is much less than the corresponding leak rate of gas. Therefore, even if a leak path developed, the flow rate capacity of the pressurization system should be adequate to compensate for the leak.
2. By maintaining a gas pocket in the model, the pressurization system used for the LST, with nitrogen gas as the pressurization medium, could be used for the SFMT without any major modifications. The only modification required would be installing additional piping inside the model to allow the gas to be introduced at the dome apex and to fill (and drain, if necessary) the model. Reducing the volume of gas to be pressurized lowered the demand on the pressurization system in the event of a leak, as well as the volume of gas required to conduct the test. In the

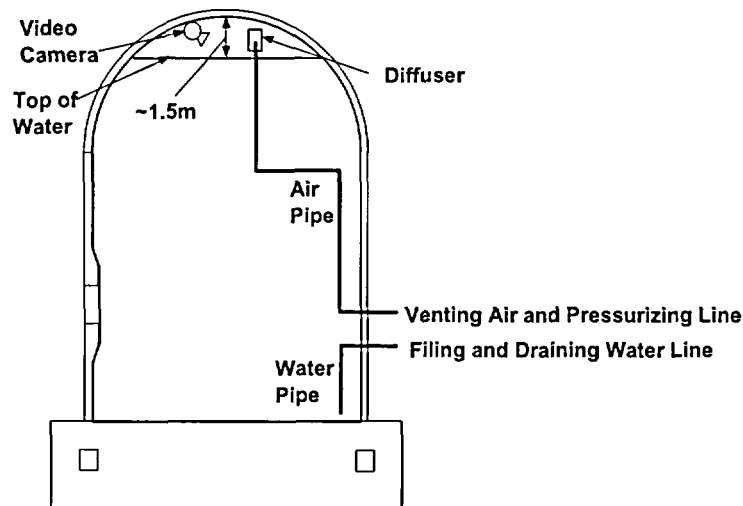


**Figure 5.24 PCCV Structural Failure Mode Test Concept**

case of the SFMT, a pressurized tube trailer could be used instead of the more expensive liquid nitrogen source required for the LST.

3. Since the pressurization system could compensate for small leaks, it is not essential that the elastomeric liner be completely leak-tight, only that the leaks would be small enough to allow the model to be pressurized to the desired level.
4. Water leaks would be readily visible, compared to gas leaks.
5. In the event of a catastrophic PCCV model rupture, the energy stored in the model nearly filled with water is much less than the stored energy if pressurized to the same level with gas. As a result, the safety exclusion zone around the model could be reduced, if necessary.

At the same time, filling the model with water would have some disadvantages:

1. Any instruments or other electrically-powered components (lights, cameras, etc.) inside the model would have to be removed or completely sealed.
2. The internal pressure would not be uniform due to the hydrostatic head, approximately  $1.4 \text{ kg/cm}^2$  (20 psig).

These disadvantages, however, were not deemed significant, and efforts focused on selection of a suitable liner. A number of vendors were contacted, and two proposals for sealing the liner were considered. One proposal was to prefabricate a 5 mm (200 mil) PVC sheet liner, which would be installed inside the model by heat welding the seams and sealing around the penetrations using ring clamps. The second proposal was to spray on a two-part polyurea coating, also a minimum of 5 mm (200 mil) thick. After considering both proposals, the sprayed-on lining was selected since it could be more readily adapted to the irregular liner surface and had significant cost and schedule advantages. The elastomeric liner was installed by Ershigs Corporation<sup>31</sup> in August, 2001 after the interior model inspection was completed and all the surface instrumentation was removed. The application of a test sprayed-on liner is shown in Figure 5.25.

After the elastomeric liner was installed, the interior instrumentation for the SFMT was installed. A reduced set of instruments was selected, allowing one data acquisition computer to scan all the gages in less than 60 seconds to support 'rapid' pressurization of the model. The instrumentation suite for the SFMT consisted of the following (A complete list of all the SFMT gages is provided in Appendix H):

<sup>31</sup> Ershigs, 742 Marine Drive, PO Box 1707, Bellingham, WA 98277, ( <http://www.ershigs.com/> )

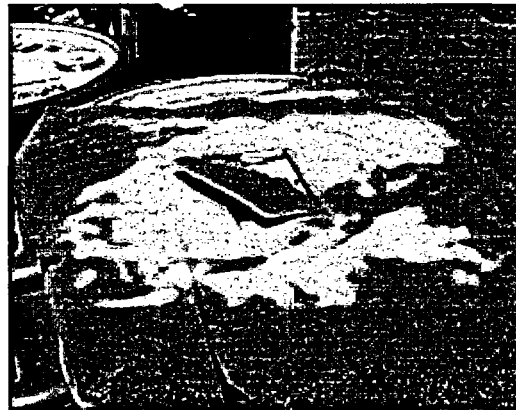
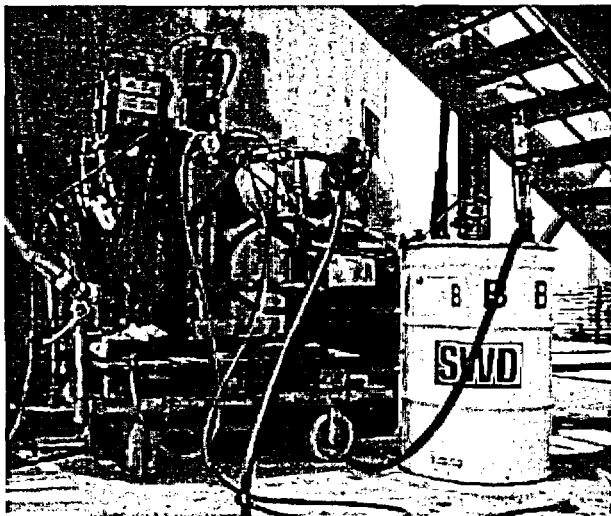


Figure 5-25. Test Specimen of Elastomeric Lining

1. All interior gages used for the LST were removed or abandoned. These were replaced by 20 waterproof LVDTs, 17 radial and three vertical, located as shown in Figure 5.26.
2. Five interior pressure transducers, three below water at the base, cylinder mid-height, and springline, and two to measure the gas pressure.
3. Two interior video cameras and lights to monitor the E/H and the water surface.
4. 18 exterior liner strain gages
  - a. 14 at meridional at wall-base junction
  - b. Four at hoop stiffener details
5. 82 rebar strain gages (Standard Output Locations (SOLs)).
  - a. 35 rebar gages (all 22 SOL plus 13 meridional at wall-base junction)
  - b. 47 gage bars (all surviving)
6. All surviving tendon strain gages and all load cells.
7. Soundprint® acoustic monitoring (external sensors only).
8. Concrete strain (six SOFO gages).
9. Four external digital video cameras at 0 degrees, 90 degrees, 270 degrees, and 360 degrees, completely covering the PCCV cylinder wall.



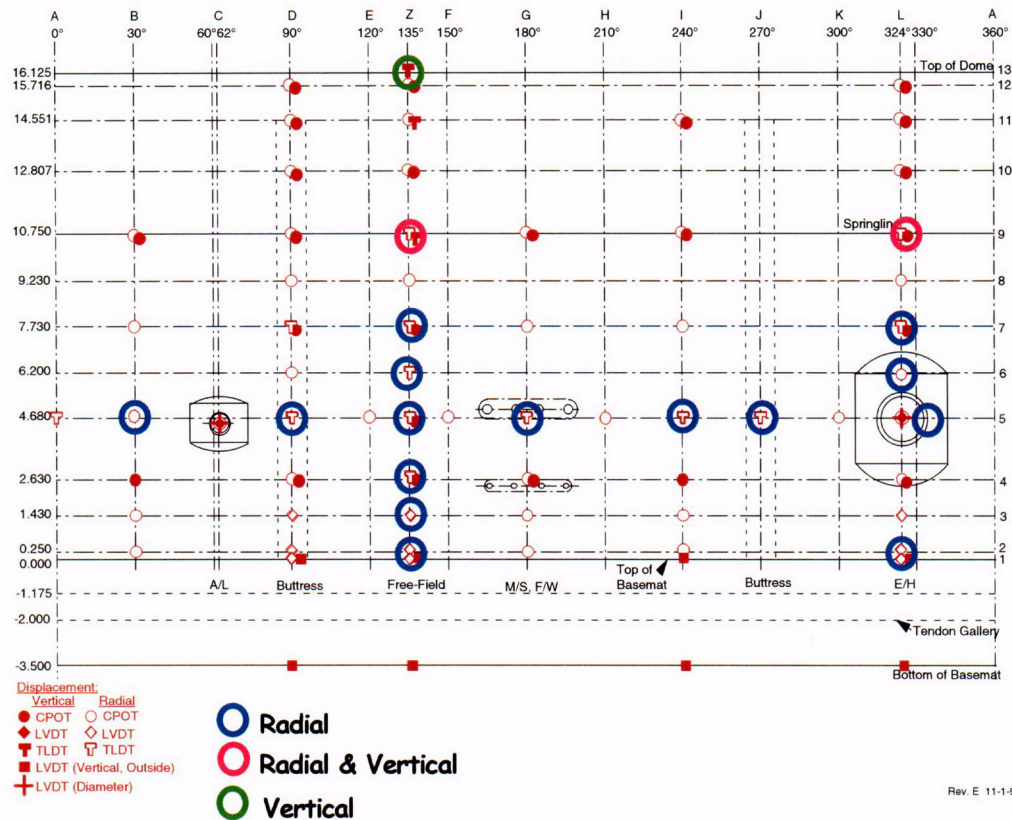
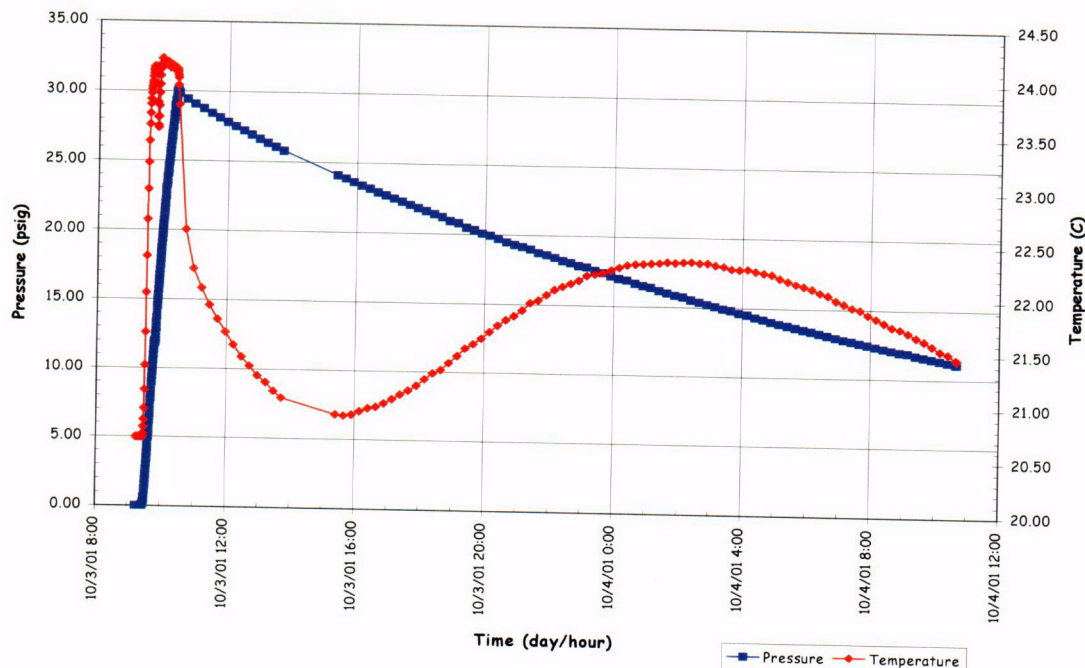


Figure 5.26 SFMT Displacement Transducer Layout

After completing the installation and all test-readiness checks, the E/H cover was installed and sealed. A low pressure pneumatic test was conducted to check for leaks on October 3, 2001. The pressure and temperature time histories for the leak test are shown in Figure 5.27. The leak test began at approximately 09:30 and a leak was detected (via the acoustic system) at approximately 0.2 Pd (~12 psig). Pressure was increased to the target pressure of 0.5Pd (30 psig), at which time the vessel was isolated and monitored for a 24-hour leak test. The acoustic system (multiple sensors) continued to output signals consistent with a leak in the model and several potential leak locations were identified.

Once the model was deemed stable, the nitrogen supply was isolated and a close inspection of the model was conducted. Through a combination of visual/auditory inspection, hand-held acoustic monitoring, and the application of soap-water solution, a number of locations were discovered where nitrogen gas was leaking from the model.

- The largest apparent leak was from a crack on the left-hand side of the 90-degree buttress at an elevation of approximately 6 m (20') above the top of the basemat (Level 6 in the cardinal coordinate system). This leak was the first detected by the acoustic system and was immediately confirmed during the close-up inspection.
- Secondary leaks, identified by the acoustic system, were confirmed at 150 degrees/3 and 6 m (10 and 20') and 210 degrees/4.5 m (15'). These leaks appeared to be through previously existing cracks in the concrete. The leak at 150 degrees was along the horizontal construction joints between C1, C2, and C3 as well as along a vertical crack extending between C2 and C3. The leak at 210 degrees also appeared to be through a previous crack.
- The acoustic system also suggested leaks at 300 degrees/1 to 2 m (3 to 6-1/2') and 360 degrees/0 m, but close-up examination could not confirm leakage at either location.
- During the close-up inspection, a leak was also detected at 30 degrees/5 m (16') which was not initially identified by the acoustic system.
- Close-up inspection of the penetrations also revealed leakage at the F/W penetrations. There was no evidence of leakage at the E/H, A/L, or M/S penetrations.



**Figure 5.27 Pre-SFMT Leak Test Pressure and Temperature**

These results indicated that, in spite of the manufacturer's quality control procedures coupled with detailed visual inspection (individual locations that appeared suspect were also sealed with silicone sealant prior to closing the model), the sprayed-on liner was not impermeable. Once the gas escaped through the sprayed-on and steel liners, it migrated between the steel and concrete until it found an exit path. The pressure did not appear high enough to tear the sprayed-on liner when a leak was first detected.

The calculated leak rate, shown in Figure 5.28, was initially 70% mass/day at the maximum pressure of 2.1 kg<sub>f</sub>/cm<sup>2</sup> (psi) decaying to 45% at 0.77 kg<sub>f</sub>/cm<sup>2</sup> (11 psi) over 24 hours. The sound levels as detected by the SoundPrint system (shown in Figure 5.29), which are roughly proportional to the rate of gas escaping, indicated a stable leak rate that was, to a large extent, independent of the pressure.

Based on these results, it was concluded that the leak was most likely due to a pre-existing hole(s) in the sprayed on liner which did not increase (or decrease) significantly during pressurization or during the leak test. (The equivalent orifice size reduced from about 6 mm (0.25") at 2.1 kg<sub>f</sub>/cm<sup>2</sup> (30 psi) to 5 mm (0.20") at 0.8 kg<sub>f</sub>/cm<sup>2</sup> (12 psi), based on the calculated leak rates.) As a result, the SFMT could be conducted without repairing the sprayed-on liner while maintaining a reasonable chance that the leak would not grow significantly and overwhelm the capacity of the pressurization system. (Nevertheless, during an unscheduled one-month postponement of the SFMT, the surface was retested with a 'spark-tester,' and a few small holes were discovered and sealed. The model was then resealed and readied for filling with water.)

Filling the PCCV with water and the SFMT began at approximately 09:00 November 6, after the initial data scan was taken, and continued until November 8, 2001. Slow water leaks were initially observed late November 6, after the model was about one-quarter full, however, the amount of water leaking was insignificant. The pressure time histories at various elevations in the model from the start of filling to the SFMT are shown in Figure 5.30. This figure illustrates the hydrostatic head and also reflects the slight loss of water due to leaks. The water level was 'topped off' on November 12, prior to the start of the SFMT.



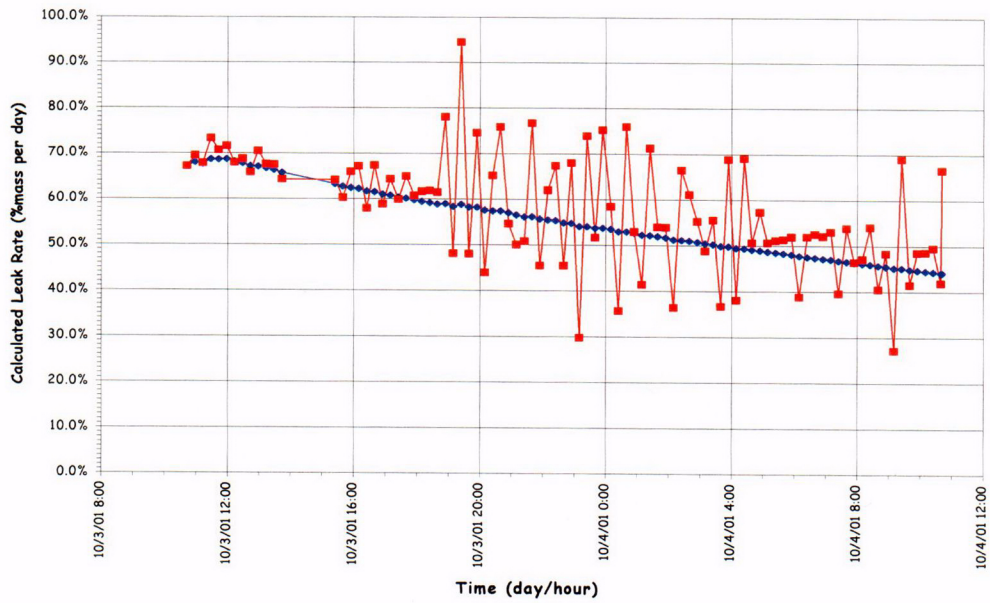


Figure 5.28 Pre-SFMT Leak Rate Test

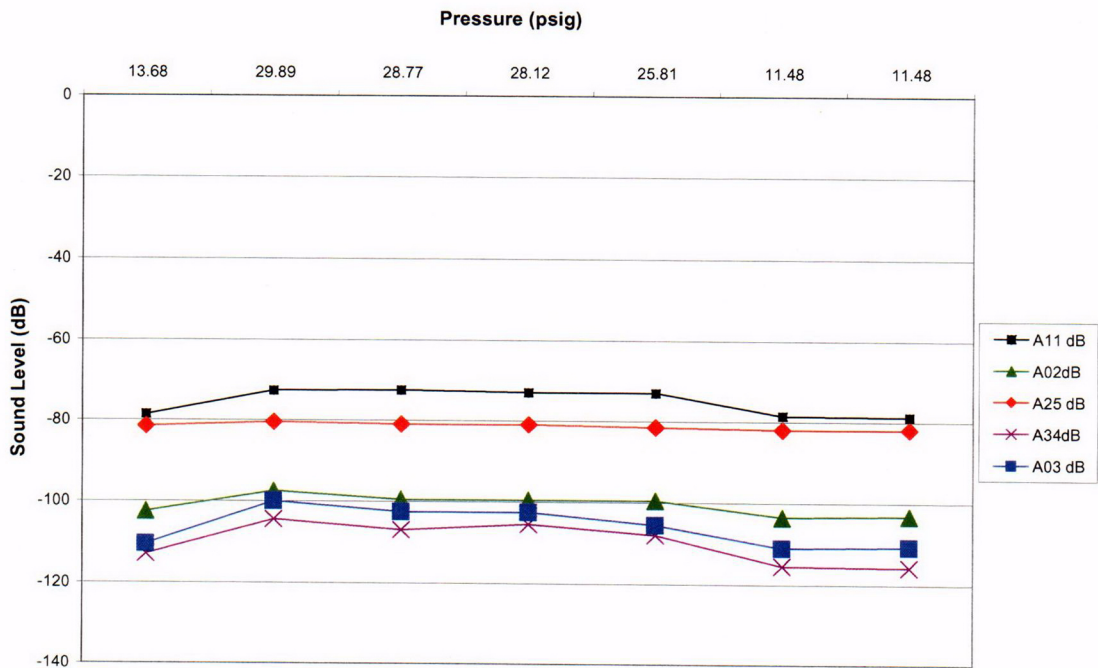


Figure 5.29 Pre-SFMT Leak Test Acoustic Data



**Figure 5.30 Pre-SFMT Hydrostatic Pressures**

The test sequence planned for the SFMT was to rapidly pressurize the model using nitrogen gas to compensate for the known leaks in the model. The minimum flow rate capacity of pressurization system, 14 std.m<sup>3</sup>/min (500 scfm), would increase pressure in the reduced void space at a rate of about 0.35 kg<sub>f</sub>/cm<sup>2</sup> (5 psi) every minute. At this rate, the model could be pressurized to failure in less than an hour.

The SFMT began shortly after 10:00 AM on Wednesday, November 14, 2001. The pressure time histories are shown in Figure 5.31. The pressure time history of all five gages are shown along with the effective model pressure, which is calculated as a volume-weighted average. Any references to the SFMT pressures are to the effective pressure, unless noted otherwise.

The model was continuously pressurized at a rate of approximately 0.35 kg<sub>f</sub>/cm<sup>2</sup> (5psi)/min. All active sensors were continuously scanned at intervals of approximately 30 seconds and the video cameras continuously recorded the response of the model. As the pressure increased, evidence of leakage was visible as increasing wetting of the concrete surface. At 10:38 AM, the effective pressure in the model equaled the peak pressure achieved during the LST, 3.3 Pd (1.29 MPa or 188 psig). At approximately 10:39 AM, the acoustic system recorded a very high noise level event, which was interpreted as the breaking of a tendon wire. At this point in the test, events occurred very quickly. Shortly after detecting the wire break, a small spray of water was observed at approximately 0 degrees Azimuth and additional tendon wire breaks were detected by the acoustic system with increasing radial frequency. The wire break events are plotted in Figure 5.32, along with the effective pressure and the radial displacement at Azimuth L (324 degrees), elev. 6 (6280), as a function of time.

The rate of pressurization decreased and the nitrogen flow rate was increased to maintain the pressurization rate. The gas pressure and flow rates are shown in Figure 5.33. The water surface inside the model, viewed through the internal video camera, was dropping slowly, but it was unclear if this was due to leakage or radial expansion of the vessel.

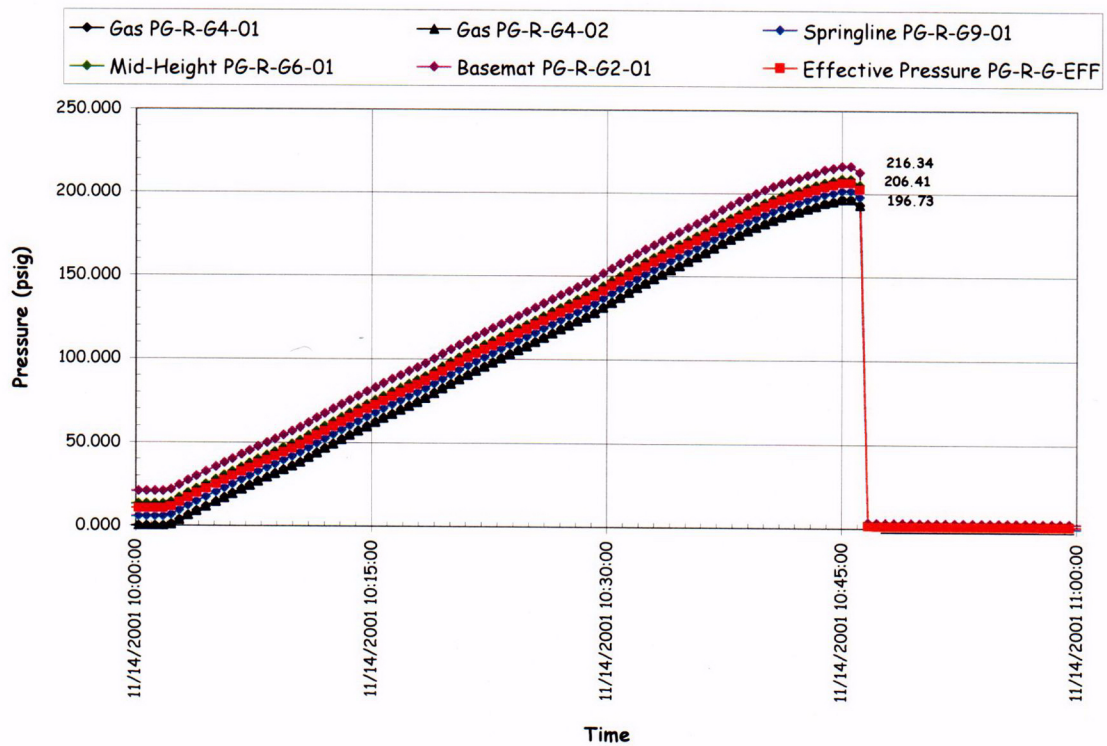


Figure 5.31 SFMT Pressure Time Histories

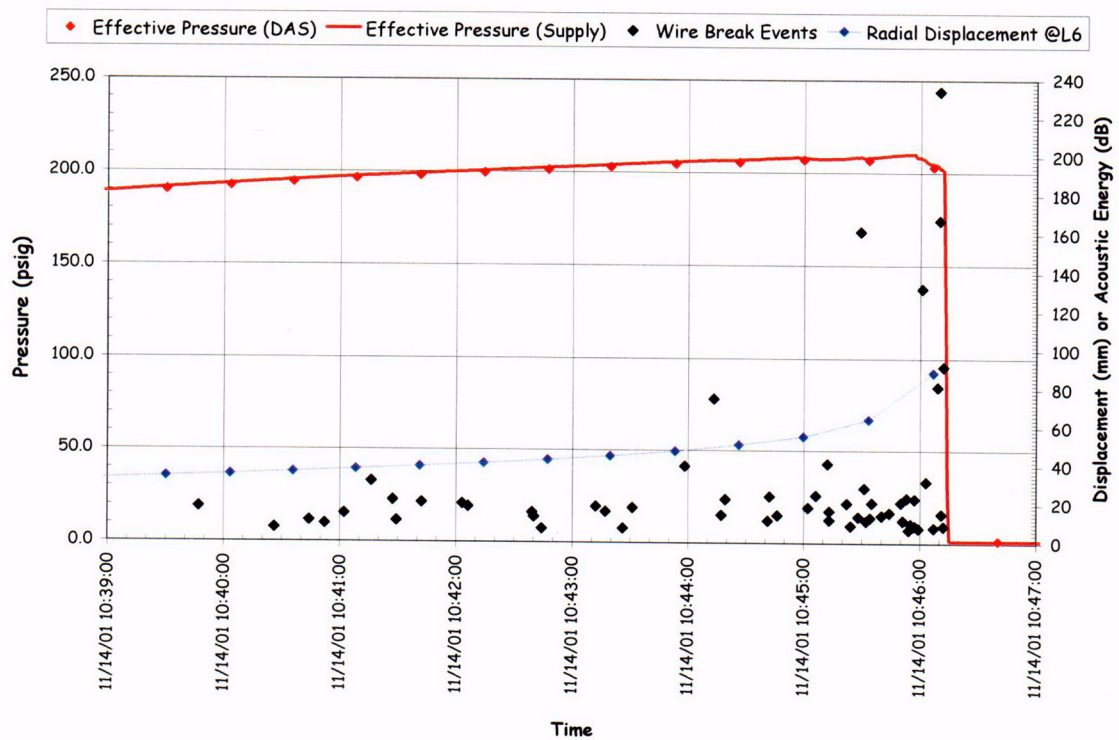


Figure 5.32 SFMT Wire Break Events vs. Pressure vs. Displacement



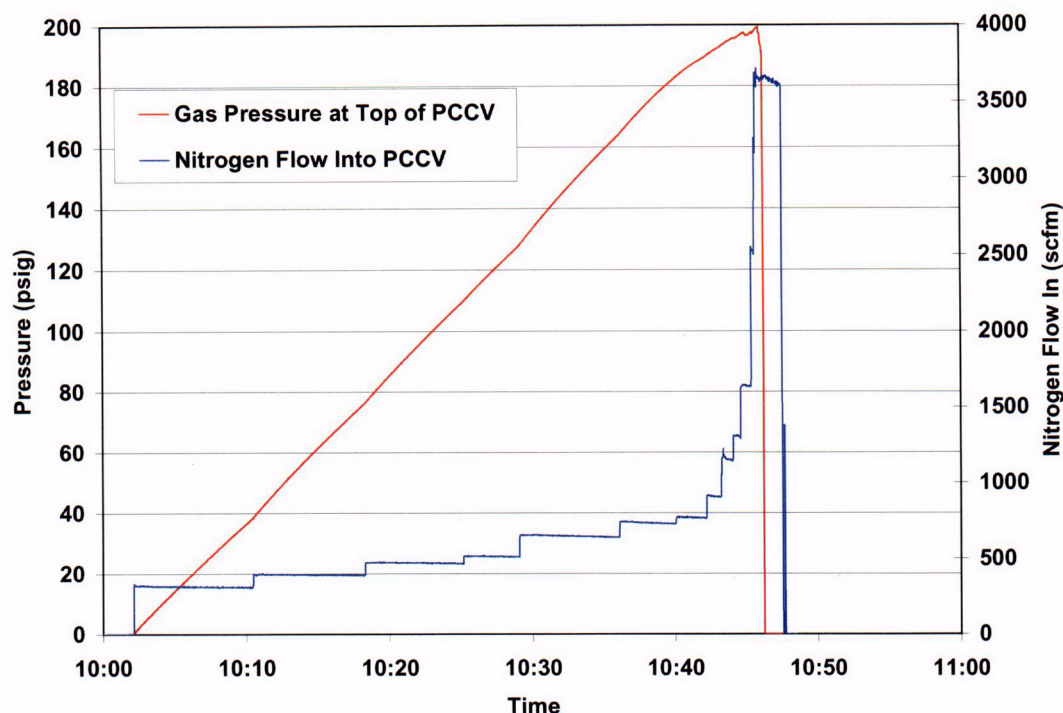


Figure 5.33 SFMT Pressurization System Data

Pressurization of the model continued until a second spray of water was observed and suddenly, at 10:46:12.3, at an effective pressure of 3.63  $P_d$  (1.42 MPa or 206.4 psig), the PCCV model ruptured violently at ~6 degrees azimuth near the mid-height of the cylinder. The rupture propagated vertically in both directions and then radiated circumferentially about 2 m above the top of the basemat, shearing off the cylinder wall. The dome and cylinder wall then came to rest on the instrumentation frame, which apparently prevented the model from toppling over. The entire collapse was over in slightly more than one second. The entire SFMT, including the sequence of rupture and collapse, was recorded by the digital video cameras. A short movie (.mpg) file showing the rupture of the model is included on the enclosed data CD. The moment of rupture is shown from all four angles in Figure 5.34. The video recorded failure of the tendons, including ejection of tendon anchors. The condition of the model after the SFMT is shown in Figure 5.35.

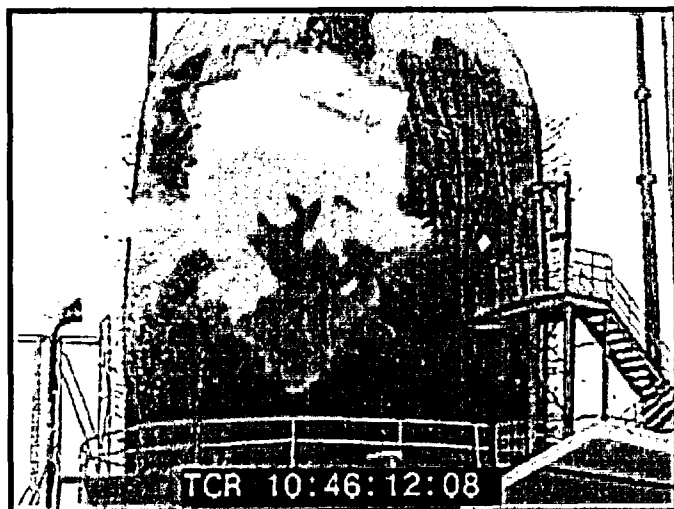
The detailed results of the SFMT are discussed in Section 5.3.3, along with observations from the posttest inspection of the model. In the case of the SFMT, posttest inspection was limited to visual inspection due to the obvious damage and restricted access for safety.

Because of program schedule constraints, demolition of the PCCV model commenced in December, 2001 and was completed in April, 2002. During this period, attempts were made to further inspect the model and characterize the damage caused by the SFMT. However, these efforts were of limited value due to the difficulty of discriminating the damage caused during the SFMT from the demolition process. A few specimens from the model were retrieved, however, more for sentimental value than for providing any further technical insight into the behavior of the model.

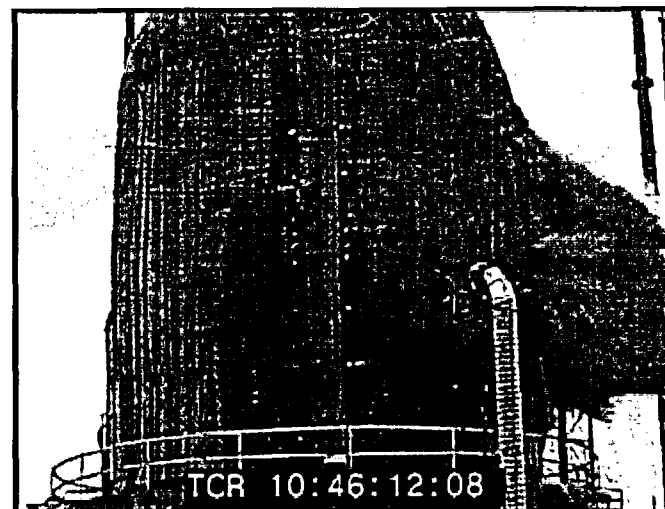
## 5.3 Test Results

### 5.3.1 Data Files

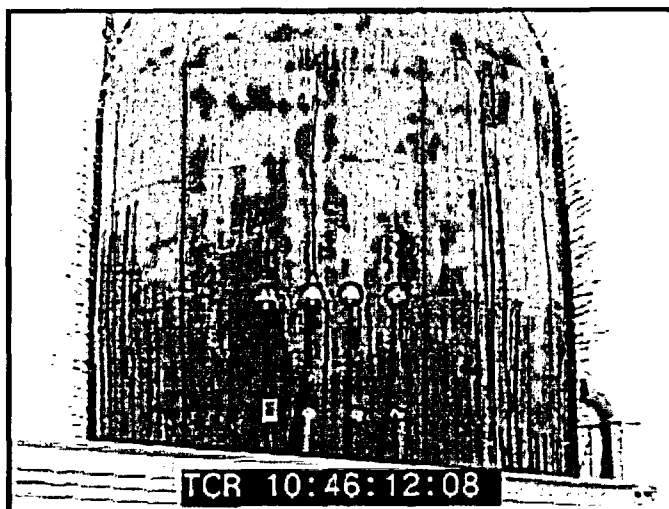
The response of the model was continuously recorded beginning March 3, 2000, prior to prestressing, through October 11, 2000, following the LST. Additional data was recorded using a modified instrumentation suite from November 6 to 14, 2001 for the SFMT. Data for each set of transducers was saved in individual files and a data management and file



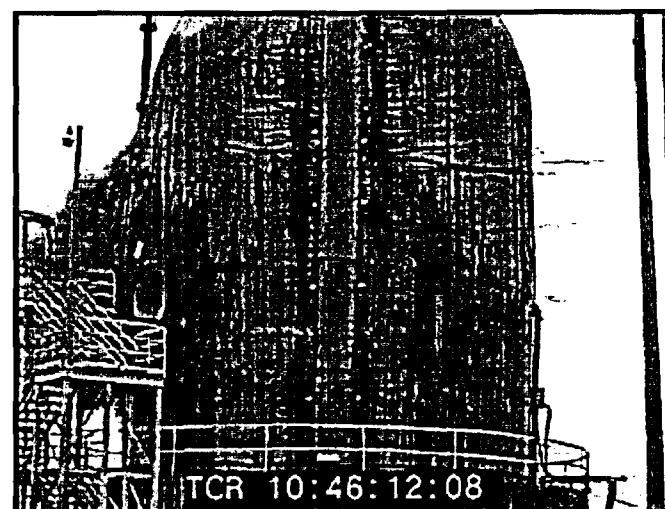
(a) 0 degrees Azimuth



(b) 90 degrees Azimuth



(a) 180 degrees Azimuth



(b) 270 degrees Azimuth

Figure 5.34 SFMT: Rupture of the PCCV Model

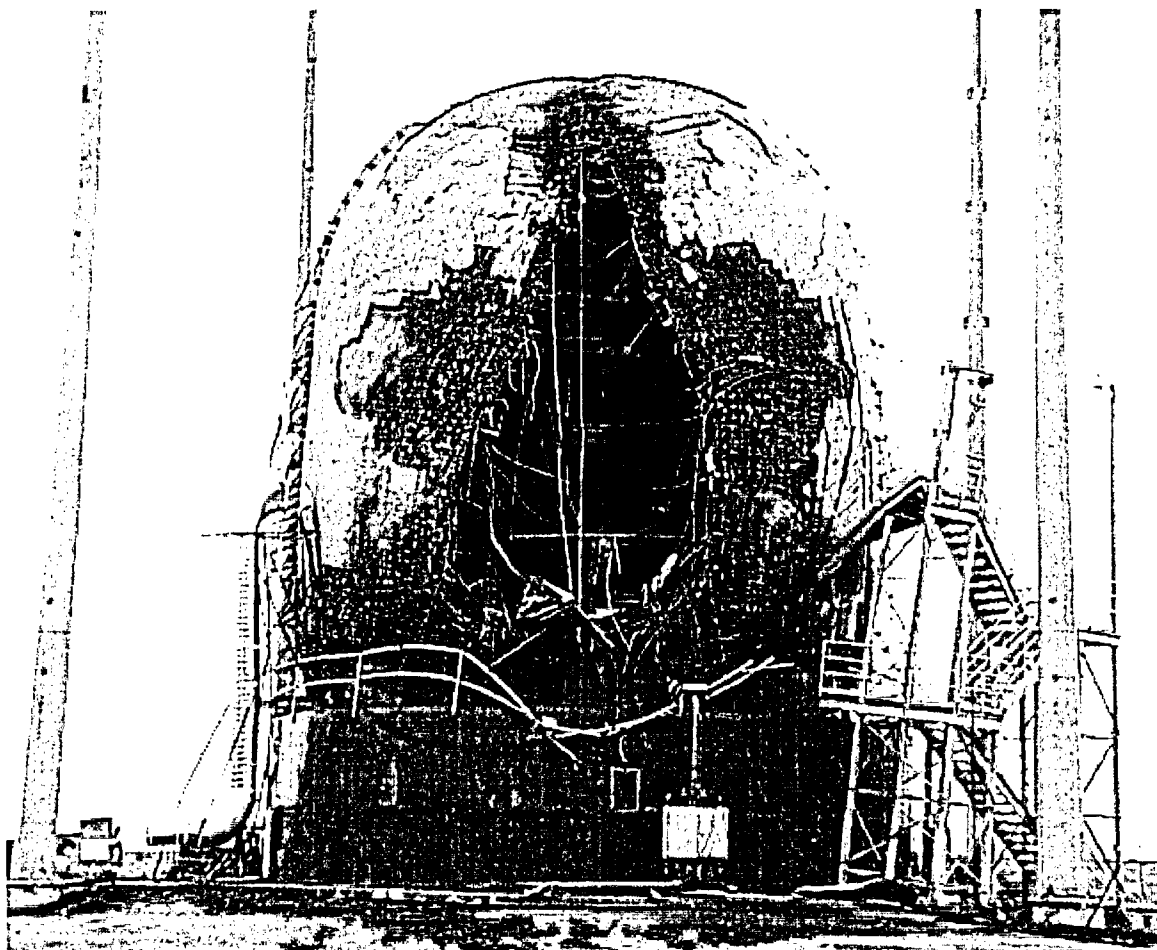


Figure 5.35 PCCV Model after the SFMT



naming scheme was developed to facilitate access and utilization of the data. A summary of the data file structure is shown in Figure 5.36.

The basic data was recorded as the output voltage (strain for strain gages, °C for temperature sensors) for each instrument at discrete time steps. This basic data is referred to as the raw, dynamic data. Note that the time reported in the data files is the DAS clock time at the start of a data scan. Since it took up to two minutes to complete a data scan (one minute for the SFMT), the actual time the data was recorded may be up to two minutes later than the recorded time. For pseudo-static loading, this is not a significant issue, but it may have some effect on the response recorded near the end of the LST and SFMT. The raw data is stored as ASCII, tab-delimited text files (.dat)

The raw, DOR is a subset of the raw, dynamic data. The concept of the DOR was defined to facilitate comparison of the data with analysis results. Typically, the analysis results are described as a function of pressure. The DOR is intended to provide a single, stable response value at each pressure step. The DOR were recorded separately from the dynamic data when the gage stability criteria (Eq. 5.1) was met, or at the direction of the test conductor.

The concept of dynamic and DOR data is illustrated in Figure 5.37. In this figure, the dynamic data during and after the LST is plotted along with the DOR for the radial displacement at the cylinder mid-height at 135 degrees. At lower pressures, the data are essentially identical; however, at higher pressures, the drift due to model creep and/or leakage is apparent. Furthermore, the DOR set does not capture the maximum pressure. In subsequent discussions of the DOR, the response at the maximum pressure from the dynamic data has been appended to the DOR for completeness.

Due to the extended length of time over which the data was recorded, the raw data files were separated into individual files by time periods. These periods were chosen to correspond with distinct loading periods, as shown in Figure 5.36. The acronyms for each period were used in the file naming scheme. The full response time history (from March 3 to October 11) for any transducer can be reconstructed by combining the data from the individual files, as illustrated in Figure 5.38 for the radial displacement at the cylinder mid-height at 135 degrees. Gaps in the data represent times when the DAS was shut down for maintenance or when temporary malfunctions (e.g. loss of power, etc.) corrupted the data. Times when the corrupted data was removed from the files are duly noted in the Excel<sup>®</sup> spreadsheets.

	Before Prestressing	Prestressing	Post Prestressing	System Functionality Test		Post SFT	SIT/ILRT	Post SIT/ILRT	Limit State Test	Post LST	Structural Failure Mode Test
	Start	End	Start	End		Start	End	Start	End	Start	End
	3/3/00	3/10/00	5/5/00	7/18/00		8/7/00	9/12/00	9/14/00	9/26/00	9/27/00	11/6/01
	3/9/00	5/5/00	7/18/00	7/21/00		9/11/00	9/14/00	9/26/00	9/27/00	10/11/00	11/14/01
	BPS	PS	PPS	SFT		PSFT	SITILRT	PSITILRT	LST	PLST	SFMT
RAW	DYNAMIC	DYNAMIC	DYNAMIC	DYNAMIC	DAS SHUTDOWN FOR MAINTENANCE	DYNAMIC	DYNAMIC	DYNAMIC	DYNAMIC	DYNAMIC	DYNAMIC
	*.dat	*.dat	*.dat	*.dat		*.dat	*.dat	*.dat	*.dat	*.dat	*.dat
	DOR	DOR		DOR			DOR		DOR		
	*.dat	*.dat		*.dat			*.dat		*.dat		
CONVERTED	DYNAMIC	DYNAMIC	DYNAMIC	DYNAMIC		DYNAMIC	DYNAMIC	DYNAMIC	DYNAMIC	DYNAMIC	DYNAMIC
	*.dat	*.dat	*.dat	*.dat		*.dat	*.dat	*.dat	*.dat	*.dat	*.dat
	*.xls	*.xls	*.xls	*.xls		*.xls	*.xls	*.xls	*.xls	*.xls	*.xls
	DOR	DOR		DOR			DOR		DOR		
	*.dat	*.dat		*.dat			*.dat		*.dat		
	*.xls	*.xls		*.xls			*.xls		*.xls		
CORRECTED									DYNAMIC		
									*.xls		
									DOR		
									*.xls		

Figure 5.36 PCCV Test Data File Matrix